AN EVALUATION OF A PASSIVELY COOLED CYLINDRICAL SPECTROMETER ARRAY IN LUNAR ORBIT
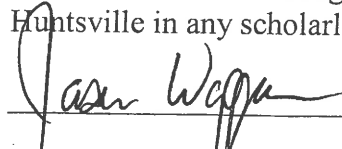
by

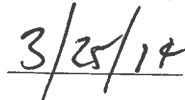## JASON WAGGONER

A THESIS

**Submitted in partial fulfillment of the requirements
for the degree of Master of Science in Engineering
in
The Department of Mechanical and Aerospace Engineering
to
The School of Graduate Studies
of
The University of Alabama in Huntsville**

**HUNTSVILLE, ALABAMA
2014**

In presenting this thesis in partial fulfillment of the requirements for a master's degree from The University of Alabama in Huntsville, I agree that the Library of this University shall make it freely available for inspection. I further agree that permission for extensive copying for scholarly purposes may be granted by my advisor or, in his/her absence, by the Chair of the Department or the Dean of the School of Graduate Studies. It is also understood that due recognition shall be given to me and to The University of Alabama in Huntsville in any scholarly use which may be made of any material in this thesis.

_____   3/25/14

(student signature)   (date)

THESIS APPROVAL FORM

Submitted by Jason Waggoner in partial fulfillment of the requirements for the degree of Master of Science in Engineering and accepted on behalf of the Faculty of the School of Graduate Studies by the thesis committee.

We, the undersigned members of the Graduate Faculty of The University of Alabama in Huntsville, certify that we have advised and/or supervised the candidate on the work described in this thesis. We further certify that we have reviewed the thesis manuscript and approve it in partial fulfillment of the requirements for the degree of Master of Science in Engineering.

_____ _Francis C. Wessling_ _3/25/14_ Committee Chair
                                    (Date)

_____ _Charles A Lundquist_ _3/25/2014_

_____ _Richard L. W_ _3/25/2014_

_____ _____ Department Chair

_____ _____ College Dean

_____ _____ Graduate Dean

iii

ABSTRACT

The School of Graduate Studies

The University of Alabama in Huntsville

Degree_____Master of Science_____   College/Dept._Engineering_____
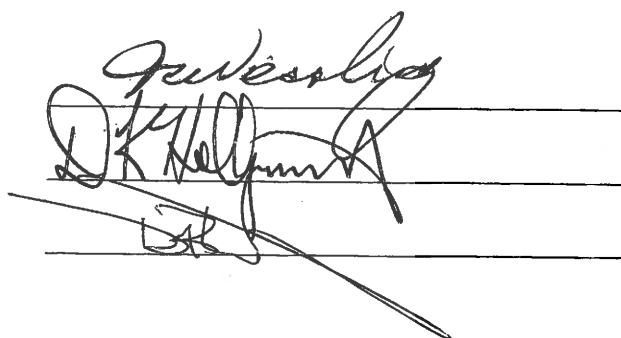
Name of Candidate _____Jason Waggoner_____

Title An Evaluation of a Passively Cooled Cylindrical Spectrometer Array in Lunar Orbit

This thesis evaluated a passively cooled cylindrical spectrometer array in lunar orbit characterizing the thermal response to provide context for decision-making to scientists and engineers. To provide perspective on thermal issues and controls of space science instruments, a background search of historical lunar missions is provided. Next, a trial science mission is designed and analyzed which brings together the elements of the background search, lunar orbit environment and passive cooling. The proposed Lunar Occultation Observer astrophysics mission which will utilize the moon for occultation in order to locate, identify and map deep space high-energy sources was chosen as the trial mission. Effort was spent sizing the array cylinder by means of a preliminary structural design. Finally, the trial science mission analysis results are provided along with the conclusions drawn. The evaluation demonstrated that the passive cooling approach allowed the maintenance of a spectrometer array below a desired maximum operating temperature.

Abstract Approval: Committee Chair _____

Department Chair _____

Graduate Dean _____

ACKNOWLEDGMENTS

It cannot be understated how much I have benefitted from the assistance, attention and insight provided by a great deal of people. I always begin by thanking my God who gives me strength and wisdom only to be followed by my patient wife and children. Second, my thesis committee (in particular the chair and advisor) has been unbelievably patient and instructive.

As this thesis pushed me in areas in which I have very little experience, my colleagues at work have demonstrated time and again why I am proud to be associated with such wonderful people and competent members of the scientific community. In no particular order of preference I list below the names of those individuals.

Brain O'Connor	Greg Schunk
Deborah Hernandez	Shawn Breeding
John Sharp	Jim Duffy
Ron Hunt	Patrick Hull
Ken Kittredge	Jeff Farmer

I would also like to mention my immediate supervisors at NASA who allowed me great lee way and were understanding as I completed this thesis.

Cynthia Ferguson

Chris Coppens

Tony Lavoie

TABLE OF CONTENTS

LIST OF FIGURES

LIST OF TABLES

CHAPTER ONE

INTRODUCTION

Presented here is an introduction to the topic of the thesis including an overview of the analysis completed and a background search of historical lunar missions. The introduction also provides a general description of the spectrometer, the main constituent parts and the problems that arise within the spectrometer due to variation in temperature.

Overview

The ultimate achieved performance for spectrometers utilized in nuclear astrophysics for high-energy photon detection is impacted by thermal control. Spectrometers which consist of inorganic scintillators and Silicon Photomultipliers (SPM) show temperature dependence with improved scintillation yield, greater energy resolution and reduced dark noise at lower temperatures. Low temperature maintenance can be achieved with active controls, yet utilization of these controls within a space science mission requires complex systems. Complex systems drive increased failure modes, system mass and cost making it desirable to passively cool spectrometers for

high-energy photon detection. This thesis will evaluate a passively cooled cylindrical spectrometer array in lunar orbit characterizing the thermal response in order to provide context for decision-making to scientists and engineers. To provide perspective on thermal issues and controls of space science instruments, a background search of historical lunar missions is provided. Next, a trial science mission is designed and analyzed which brings together the elements of the background search, lunar orbit environment and passive cooling.   Finally, the trial science mission analysis results are provided along with the conclusions drawn.

Scintillators are materials that when struck by particle radiation, absorb the particle energy which is then reemitted as light in or near the visible range. Nuclear astrophysics utilizes scintillating materials for observation of high-energy photons which are generated by sources such as solar flares, supernovae and neutron stars. SPMs are paired with inorganic scintillators to detect the light emitted which is converted into electronic signals. The signals are captured and analyzed in order to map the number and location of the high-energy sources. The SPM is utilized as it has single photon sensitivity, low voltage requirements and a fast response. SPMs are also compact, relatively inexpensive and allow the usage of lower-cost scintillating materials within the spectrometer. These characteristics permit large-area arrays while lowering cost and power requirements.

The ability of a spectrometer to record and identify the interaction of high-energy photons for scientific return is not a trivial matter. Background noise is generated when particles that have not originated from the desired distant source impact the spectrometer. Additionally, thermally induced electrical signals are randomly generated within the SPM

even in the absence of light which is referred to as dark current. Overcoming these obstacles requires greater light emittance and energy resolution with reduced dark current. Strong scintillation photon emittance ensures that low energy impacts will produce enough visible photons to be detected by the SPM. Higher energy resolution will ensure that single photon impacts can be distinguished from others of similar wavelength and energy; reduced dark current decreases the generation of random signals not associated with a photon impact. Increasing efficiency in each of these properties in a spectrometer comprised of inorganic scintillators and SPMs requires low temperatures. Low temperature maintenance in a lunar environment presents many unique challenges of its own.

Even with the accumulated successes of past missions, the lunar environment remains a thermal challenge for engineers. The lunar orbit thermal environment is driven by radiation from three sources, direct solar radiation, reflected solar radiation from the lunar surface (albedo) and lunar radiation (Clawson 2002). Direct solar radiation values are consistent with those seen in Earth orbit (1325 W/m^2) (Clawson 2002). The percentage of solar radiation reflected from the moon is consistently very low with the moon's dark regolith covered surface absorbing nearly 90% of the incident light (Clawson 2002). Yet, it is this absorption that gives the lunar orbit environment one of its most difficult thermal attributes as the absorbed solar radiation is released from the lunar surface as infrared radiation (IR). IR is of a wavelength that is readily absorbed by surfaces designed to function as radiation emitters. It is practical to therefore "choose radiator locations and spacecraft attitude to minimize radiator views to the lunar surface, when possible…pointing the radiator towards the sun to some extent, to minimize its

3

view to the lunar surface, is frequently preferable. (Clawson 2002)" Additionally, the amount of direct solar radiation, lunar IR and albedo an orbiting satellite receives varies from one side of the moon to the other as the moon blocks the sun from view. This environment produces large temperature variations in a satellite's instrumentation, control electronics and propulsion systems which must be understood to characterize operating temperature envelopes.

Approach

An analysis of a trial science mission is completed which brings together the elements of the background search, lunar orbit environment and passive cooling. The analysis is completed utilizing the following parameters:

1. Spectrometer Array Dimensions – dimensions of diameter and height associated with a given spectrometer layout creating the available area for observation.

2. Spectrometer Power – total power dissipated by the spectrometer consisting of the power required for operation and the power generated by dark current.

3. Lunar Orbit Parameters – orbit altitude and angle of inclination as measured from the equator.

The analysis is performed at extremes for each parameter in order to bracket the maximum design trade space open to scientists and engineers. Each parameter extreme is determined utilizing the historical background search and the constraints, both provided and derived, of the trial science mission.

The proposed Lunar Occultation Observer (LOCO) mission concept has been chosen as the trial science mission. The LOCO mission spectrometer array, consisting of individual sensor modules mounted to a cylindrical support structure, requires a low instrument temperature and has a unique thermal design challenge due to its cylindrical configuration. A working concept of the LOCO instrument is depicted in Figure 1 (R. S. Miller 2012) and highlights the unique thermal control issue of the inner surface of the cylinder being the only appreciable surface area available for rejecting heat.
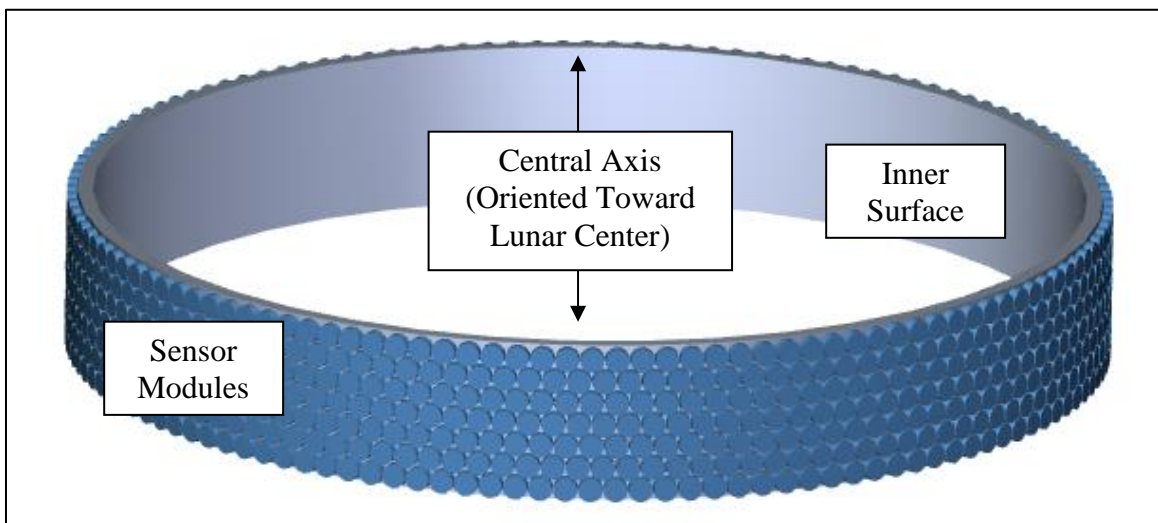
Figure 1 LOCO Cylindrical Sensor Array Concept

The surfaces most advantageous for radiators are those which have a view unobstructed by other spacecraft systems and are free from receiving radiation from other sources. By necessity, the ideal radiating surfaces for LOCO are covered with the sensor modules to form the array. The remaining surfaces are either pointed directly at the lunar surface or

are interior to the cylinder where a percentage of radiation emitted will be able to reach space while the remainder reradiates the interior surface. The LOCO mission concept, particularly the sensor module, is still preliminary in nature which precludes a detailed instrument and satellite design. The lack of fidelity requires the analysis to be completed utilizing two heat transfer assumptions:

1. Conduction Only – heat transfer only occurs between the sensor module and the array support structure through conduction.

2. Radiation Only – heat transfer only occurs from the sensor module to the array support structure by radiation.

A deeper explanation of the analysis parameters and heat transfer assumptions is provided in chapter 3 of this thesis and is introduced above to inform the reader.

Historical Lunar Missions

The following historical review provides information on unmanned missions which have operated in the lunar environment to support the example problem. The missions consisted of flybys, orbiters, surface impactors, surface landers and sample return missions. A few examples of thermal control used in lunar missions are also provided. A list of the fifty eight effective lunar missions reviewed is summarized in Table 1 (Lunar Exploration Timeline 2011) with the orbiter mission parameters summarized. The mission duration listed records the estimated time the orbiter was in its final science orbit and does not include the time taken to reach the science orbit from earth.

Table 1 Lunar Missions Reviewed

Mission	Origin	Years	Architecture
Luna 1 & 3	USSR	1959	Flyby
Luna 2 & 18	USSR	1959, 71	Impactor
Pioneer 4	USA	1959	Flyby
Ranger 3-9	USA	1962-65	Impactor
Luna 4-9, 13	USSR	1963-66	Lander
Zond 3	USSR	1965	Flyby
Lunar Orbiter 1-5	USA	1966-67	Orbiter: Low and high inclination elliptical orbits, up to 1 year duration
Surveyor 1-7	USA	1966-68	Lander
Luna 10-12, 14-15 19 22	USSR	1966-74	Orbiter: first man-made satellite of the moon
Zond 5-8	USSR	1968-70	Return
Luna 16 20 23 24	USSR	1970-76	Return
Hiten	Japan	1990	Orbiter: Highly elliptical earth orbits which passed the moon, 3 year duration
Clementine	USA	1994	Orbiter: Near polar elliptical orbits, 2 month duration
Lunar Prospector	USA	1998	Orbiter: Varying orbits including 100 km near circular polar orbit, 1.5 year duration
SMART 1	ESA	2003	Orbiter: 300 x 3,000 km elliptical, 1.7 year duration
SELENE	JAXA	2007	Orbiter: 100 km near circular polar orbit, 1.6 year duration
Chang'e 1	China	2007	Orbiter: 200 km, circular high-inclination, 1.3 year duration
Chandrayaan-1	India	2008	Orbiter: 100 km near circular polar orbit, 9 month duration
LRO	USA	2009	Orbiter: 50 km near circular polar orbit, still orbiting
LCROSS	USA	2009	Impactor
Chang'e 2	China	2010	Orbiter: 100 x 15 km elliptical, 7 month duration – left lunar orbit
GRAIL	USA	2011	Orbiter: 50 km near circular polar orbit, 11 month duration

Missions

The early history of unmanned lunar exploration began in 1958 with the majority of missions occurring in the first 2 decades of competing work between the Soviets and Americans. The Soviet Luna 2 became the first successful man-made object to impact a planetary body other than our own in 1959 (Soviet Lunar Missions 2005). However, this early success was not indicative of the decades. Thirty eight additional missions out of over 50 attempts by both nations were failures due to both launch and payload issues.

American lunar exploration during the early decades consisted of 4 programs Pioneer (probes and orbiters) (Pioneer 2010), Ranger (impactors) (Ranger 2005), Surveyor (landers) (Surveyor 2006) and Lunar Orbiter (orbiters) (Lunar Orbiter 2011). Thermal conditioning of the Pioneer probes was maintained by utilizing stripes of white paint as seen in Figure 2.

Figure 2 Pioneer Lunar Probe (Pioneer 3 2013)

The Pioneer orbiters in which the probes were transported consisted of a spherical shell

with external instrumentation, solar panels and internal propulsion. Thermal control was

to be handled by "a large number of small 'propeller blade' devices on the surface of the

sphere. The blades themselves were made of reflective material and consist of four vanes

which were flush against the surface, covering a black heat-absorbing pattern painted on

the sphere. A thermally sensitive coil was attached to the blades in such a way that low

temperatures within the satellite would cause the coil to contract and rotate the blades and

expose the heat absorbing surface, and high temperatures would cause the blades to cover

the black patterns. Square heat-sink units were also mounted on the surface of the sphere to help dissipate heat from the interior (Pioneer Space Probes 2010)."

The Ranger 9 architecture can be seen in Figure 3 with its tall conical frame topped by a cylindrical antenna mast. "White paint, gold and chrome plating, and a silvered plastic sheet encasing the retrorocket furnished thermal control (Ranger 3 2013)."
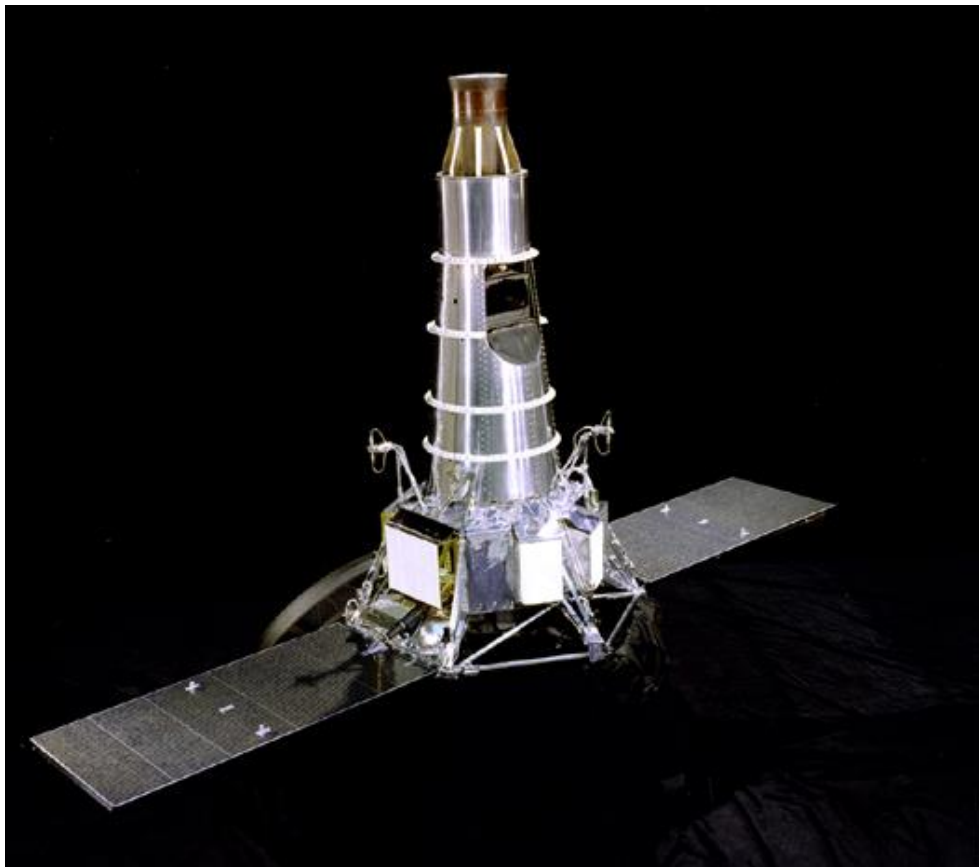
Figure 3 Ranger 9

The Surveyor and Lunar Orbiter programs provided valuable data required for the Apollo manned lunar landings. Thermal control for the landers "was achieved by a combination of white paint, high IR-emittance thermal finish, and polished aluminum underside. Two thermally controlled compartments, equipped with superinsulating blankets, conductive heat paths, thermal switches and small electric heaters were mounted on the spacecraft structure (Byers 1977)." The orbiters utilized painted surfaces, Multi-Layer Insulation (MLI) and heaters to maintain a temperature balance required for sensitive electronics unable to handle large temperature swings. Of note, the spacecraft cameras required a special "bathtub" housing to prevent the lenses from fogging and moisture build up on the film. The camera temperature was stabilized by radiating heat to the surrounding housing (Byers 1977).

The Russian Luna program encompassed the whole of mission architectures of the 4 American programs and included rovers and sample return missions. Additional thermal control approaches were utilized and focused on maintaining a set temperature range. For example, the Luna 3 was a cylindrical orbiter that provided the first pictures of the far side of the moon. "Shutters for thermal control were positioned along the cylinder and opened to expose a radiating surface when the internal temperature exceeded 25 °C (Luna 3 2013)." The active and robust lunar exploration programs of the early decades were followed by nearly 2 decades of inactivity that was rekindled in the early 90's.

The 1990s brought, in most cases, larger and far more advanced missions in the instrumentation, duration and precision of mission profile. The new missions focused on orbiters and sample returns. Additionally, other countries began to participate in lunar

exploration including Japan, China and India. The thermal control systems were passive in nature for almost all of the orbiters with the exception of powered louvers or doors and survival heaters. In the 1990s Hiten, Clementine and the Lunar Prospector seen in Figure 4 (Lunar Prospector 1998) utilized a smooth or faceted cylindrical body covered in solar panels and rejected heat through radiation panels. It should be noted the Lunar Prospector was spin-stabilized preventing a single surface from being constantly heated by external sources.
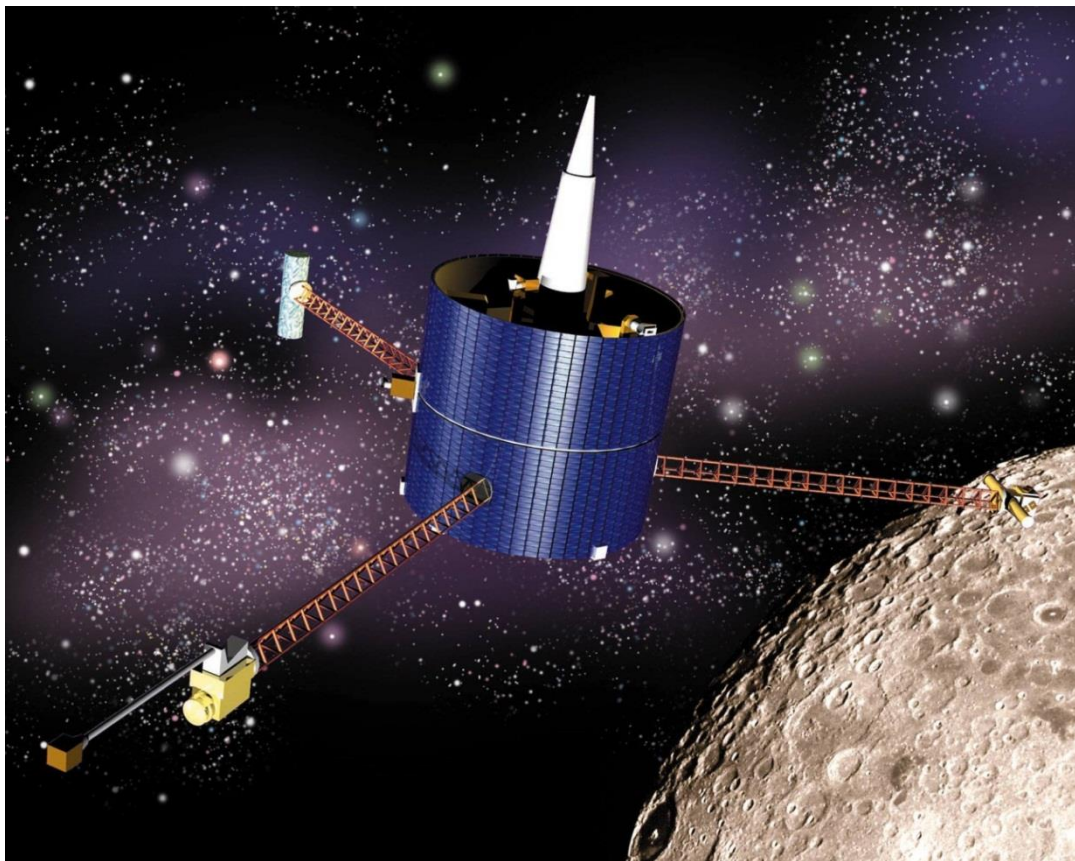
Figure 4 Lunar Prospector

The programs of the 2000s, including the Lunar Reconnaissance Orbiter (LRO) seen in Figure 5 (Lunar Reconnaissance Orbiter 2009), were found to be covered with sensitive instruments and electronics. They required a proactive thermal design approach which drove the use of avionics sections or modules. For example, LRO sensitive components were co-located along with large thermal masses and heaters which could pre-heat the electronics prior to the orbiter being shaded from the Sun by the moon (Baker, Cottingham and Peabody 2011). Additional consideration was given to the location and positioning of MLI and targeted radiators for each science instrument.
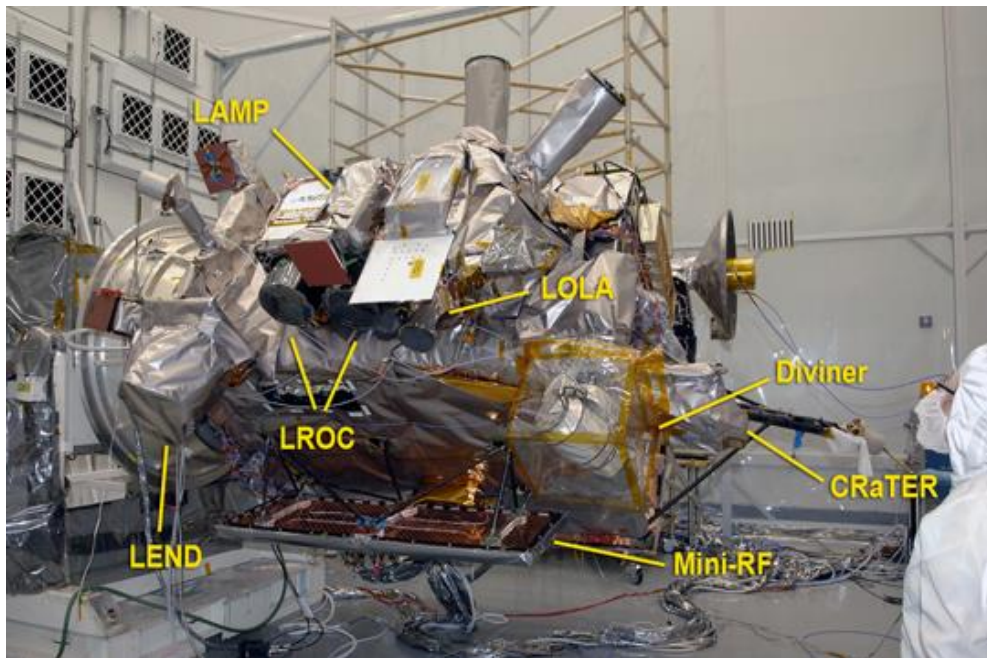
Figure 5 LRO Instrumentation

Conclusions

The historical lunar mission review demonstrated the complexity of maintaining avionics and instrumentation within a desire range. Passive thermal control approaches were successfully utilized but in most cases, thermal heaters and thermal mass were required to maintain instruments within a specific thermal operating range. After a 15 year period of no activity, lunar missions again were completed with an emphasis on orbiters. Elliptical and circular orbits were utilized. The circular orbit altitudes ranging from 50 to 200 km and were high-inclination or near polar in nature (Table 1).

CHAPTER TWO

CASE STUDY

Presented here is the design of the trial science mission which brings together the elements of the background search, lunar orbit environment and passive cooling. The provided constraints of the trial mission as well as those derived to ensure a relevant and adequate analysis are also presented. The derivation provides a description of structural design assumptions and details gathered from a computer model of the array cylinder. The additional structural design work is performed to illustrate a realistic cylindrical spectrometer array design as it is directly applicable to the creation of the thermal analysis.

Mission Background

The LOCO nuclear astrophysics space science mission concept has been chosen as the trial science payload to characterize the effectiveness of a passive approach to thermal control. This concept was chosen as it is a real application which encompasses the primary thesis objectives of a passively cooled cylindrical spectrometer array in lunar orbit. LOCO will perform an all-sky survey intended to investigate a variety of phenomena including but not limited to star formation rates, solar flares and potential

dark matter annihilation processes. Achieving these goals requires a rigid set of

instrument design requirements traditionally met with "complex, position sensitive

detectors that traditionally operate in the hard X-ray or nuclear γ-ray regime." (R. Miller

2010) LOCO proposes to meet the design goals by employing a large area spectrometer

array while utilizing the moon as a large body for occultation. A best effort is made in

the thesis to determine an overall structural design approach for the spectrometer array to

provide a realistic analysis. The occultation process will capture each time a distant high

energy source is eclipsed by the moon along with the corresponding spacecraft position.

Advanced image analysis and statistical methods will be used to identify distant sources

and catalog source locations from the captured data.

The LOCO spectrometer array is comprised of individual sensor modules of

inorganic scintillator crystals, SPMs and the necessary signal processing electronics.

Each sensor module is positioned to create faceted rows on the outer lateral surface of a

cylinder whose long axis is oriented at the lunar center of gravity. The configuration will

provide a large array area with increased sensitive area in the high-energy source

direction and minimal sensitive area in the lunar surface direction. A notable

characteristic of the LOCO sensor module is that "operating temperature is a key

motivating factor…in order to reduce thermal-induced dark noise in sensitive

electronics... (D. R. Miller 2008)." Minimizing operating temperature will also provide

increased light emittance from the inorganic scintillating material as well as greater

energy resolution to separate and identify unique high-energy sources. The thermal-

induced sensitivity requires each individual sensor module to operate below a maximum

temperature limit, 0° C (D. R. Miller 2008). A minimum operating temperature limit is not defined.

The majority of the effort performed regarding the LOCO concept has dealt with the performance and architecture of the spectrometer array as it is the fundamental instrument of the mission. Spectrometer component materials, sizing and electronics have been selected and tested but final packaging is not complete. Additional work completed included a study in 2009 by Ball Aerospace on mission architecture concepts. The study focused on preliminary mass budgeting, trajectory analysis, propulsion system constraints and overall layout. The preliminary mass budget was created using the mass and cost constraints of commercial launch vehicles as well as available satellite buses.

System Design

The LOCO space science mission consists of two main components: the spacecraft bus and the cylindrical sensor array. The spacecraft bus contains all of the elements required for a fully functioning orbiting satellite including communication, power and propulsion systems. The cylindrical sensor array is comprised of a number of individual spectrometer modules and the cylindrical structure on which they are mounted which will double as a radiator surface for the thesis. The architecture utilized for the analysis is defined in the following manner and is shown now for reader clarity (see Figure 6).

1. Array Cylinder

   The spectrometer array cylinder is the structure upon which all the individual spectrometer modules are mounted and aligned in multiple rows about the circumference. The cylinder height is a function of mass limits.

2. Sensor Module

   The sensor module is a "black box" of known size and power requirements. Each sensor module is an individual spectrometer consisting of inorganic scintillator material, SPM and signal processing electronics. Multiple sensor modules are required to create a large-area array.

3. Disk

   The Disk is a surface that covers the cylinder opening closest to the lunar surface. It is used to represent a commercial off-the-shelf (COTS) satellite "bus" which contains all of the elements required for a fully functioning orbiting satellite. The sizing and location of the Disk will be explained in greater detail in following sections.

CROSS SECTION		BOTTOM ISOMETRIC VIEW

Array Cylinder

Inner Diameter (ID)

Outer Diameter (OD) (Modules not Shown)

Sensor Module Rows

DISK

Disk
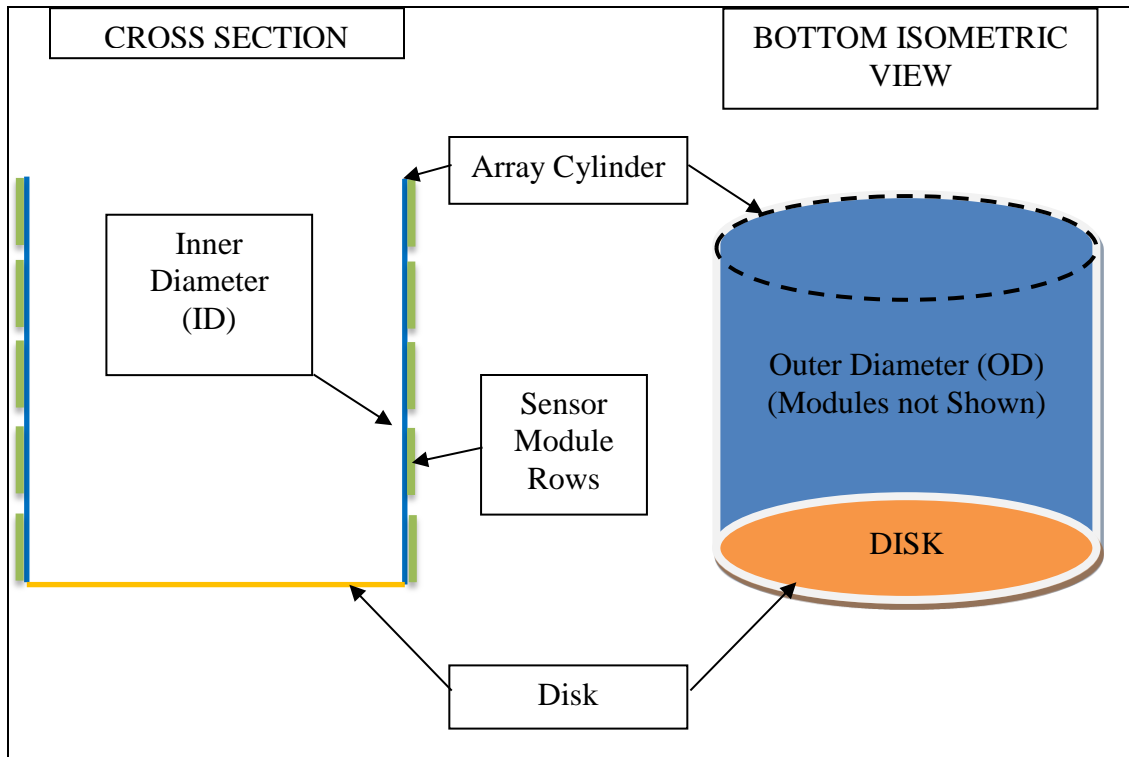
Figure 6 Architecture Nomenclature

Constraints

A passive thermal control approach for the spectrometer array is desired to minimize the cost, mass and failure potential associated with complex, active thermal control systems; passive control array designs will be presented only. A passive thermal control system is one with no pumped or commandable thermal control hardware such as fluid loops or thermoelectric coolers. Additional constraint will be added to exclude the use of any movable sun shields (shutters and louvers) and heat pipe systems even though both approaches can be designed without any need for active control. The strictness of

the definition drives the evaluation to be concerned only with results obtained due to array geometry, spectrometer power levels, material properties and the application of thermal coatings and multi-layer insulation (MLI).

In addition to the passive thermal assumption, applicable evaluation constraints and requirements were provided by the LOCO Principal Investigator (PI). These include mass, cost, array geometry, sensor module characteristics and science mission parameters. The constraints are utilized as the basis for the analysis including any thermal modeling decisions made and additional parameters derived.

Mass

Of primary consideration is the total available mass for the complete sensor array which must include the mass of each individual sensor module within the array as well as the array structure. The sensor module mass as provided by the LOCO PI is .868 kg (R. S. Miller 2012). The available array cylinder mass is a function of the launch vehicle chosen and the corresponding vehicle capability. The Ball Aerospace trade study, provided by the PI, included a breakdown of launch capabilities per vehicle system and the mass available for the complete sensor array (Max Instrument Mass in Figure 7) once considerations such as margins, spacecraft fuel and vehicle wet mass were taken into account. The results of the trade study are shown in Figure 7 (Bank and Ebbets 2009).

Bi-Prop System						
Isp (seconds)	300.00					
Required delta-V (m/s)	1000.00					
Launch C3 (km2/s2)	-1.96					
Spacecraft dry mass (kg)	200.00					
	Delta IV (5m Fairing)	Atlas V (551)	Atlas V (401)	Atlas V (501)	Falcon 9 (5m Fairing)	Taurus 2 (4m Fairing)
Launch Capability (kg)	9500	6500	3600	2800	2000	1260
30% Margin	2192	1500	831	646	462	291
SC Wet Mass @ Launch (kg)	7308	5000	2769	2154	1538	969
SC + instrument dry mass (kg)	5202	3560	1971	1533	1095	690
Max Instrument Mass (kg)	**5002**	**3360**	**1771**	**1333**	**895**	**490**
Fuel (kg)	2105	1440	798	620	443	279
Percent Fuel	29%	29%	29%	29%	29%	29%

Figure 7 Ball Aerospace Mission Concept Study Summaries

Cost

Of the systems investigated, only the Falcon 9 and Taurus 2 launch vehicles are applicable. Each vehicle meets the cost constraints of the National Aeronautics Space Administration (NASA) Middle-Class Explorer (MIDEX) mission which is the LOCO proposal class.

Array Geometry

The spectrometer geometry chosen for this thesis is one of a cylindrical configuration with an instrumented outer surface whose axis is oriented at the lunar center. The diameter and height of the cylinder is constrained by the allowable launch vehicle payload volume driven by the vehicle fairing sizes. The launch vehicle fairing sizes are shown in Table 2 .

Table 2 Launch Vehicle Fairing Geometry Constraints

Constraint	Value	Comment
Falcon 9 (2009)		
Maximum Payload Diameter	4.6 m	Driven by dynamic envelope
Maximum Payload Height	6.6 m	Maximum height with consistent cross section
Taurus II (2010)		
Maximum Payload Diameter	3.4 m	Driven by static envelope
Maximum Payload Height	4.2 m	Maximum height with consisten cross section

Sensor Module

Three sensor module characteristics, in addition to mass, were provided that affect the

thermal analysis. The characteristics are the sensor dimensions, power dissipation and

operating temperature range. Each characteristic is summarized in Table 3 along with the

sensitive instrument area per sensor module.

Table 3 Sensor Module Charateristics

Constraint	Value	Comment
Sensor Module		
Power Dissipation Per Module	.086 Watts	Required for operation and generated by dark noise
Module Dimensions	.093 x .093 x .04 m	Based on a 3x3 array of silicon photomultipliers
Maximum Operating Temperature	0° Celsius	
Minimum Operating Temperature	N/A	No limit set for cold case
Mass Per Module	.868 kg	
Sensitive Area Per Module	.006 m^2	

Science Mission Parameters

Four mission parameters were provided that affect the thermal analysis. These

parameters are field of view measured below the cylinder array surface closest to the

lunar surface, total sensor array area, orbit altitude and orbit angle of inclination as

measured from the lunar equator. The field of view affects the overall system

architecture as system components cannot be located such that a sensor module view to

space and the lunar surface is obstructed. The total sensor array area is desired by the PI

in order to meet science objectives and is provided for clarity. The orbit altitude and

angle of inclination affect the amount of direct solar radiation, reflected solar radiation

and lunar IR the sensor array receives. The provided mission parameters are summarized

in Table 4.

Table 4 Mission Parameters

Constraint	Value	Comment
Field of View (FOV)	71° Below Array Horizon	Horizon defined by plane created by the Disk
Total Area[*]	4 m^2	Desired to achieve required sensitivity
Orbit	Circular with 75° angle above equator	Lunar and near polar
Altitude	100 km	

* Provided for clarity

Array Cylinder Sizing

The constraints provided left two primary gaps in knowledge, namely the array cylinder structural design approach and how to account for the spacecraft bus. The structural design approach is pertinent for three reasons: (1) the design must provide mounting provision for each sensor module while maximizing available radiator surface area, (3) the array must remain within mass constraints and (3) the structural design must be adequately represented within the thermal model. The structural design work is ultimately performed to illustrate a realistic cylindrical spectrometer array design adding credence to the results.

The spacecraft bus (Disk) provided a model integration problem. A functional satellite requires avionics, control, power and propulsion for a start. These components reject or require heat and must be structurally connected in some manner to the cylinder array. Also, the viewing requirements of the sensor array constrain the location of the components along the cylinder central axis. Placing the satellite components at the top of the cylinder would close radiation paths to deep space. Placing the components within the cylinder would require a detailed knowledge of the components and sizing of the array. The ideal location for the evaluation is to assume the components are at the opening facing the lunar surface to shield the inner diameter from lunar IR which would be readily absorbed by the radiators. The disk diameter will match the cylinder diameter to prevent lunar IR from reaching the inner cylinder surfaces.

The modeling design space for each thermal analysis model began with fully utilizing the maximum available payload fairing diameter. The largest available cylinder

diameter allows the total array area to be increased through growing the height of the cylinder and adding additional sensor module rows until a total mass limit is reached. Also, the available area at the top of the cylinder through which radiation could reach space increases with the square of the diameter. The increased area was of importance as the Disk covers the bottom of the cylinder blocking one path by which radiation could reach deep space.

Array Cylinder

Much design consideration was given to the construction and material choice for the cylinder array assumed within the thermal analysis models. A detailed assumption was necessary for three primary reasons; (1) the array cylinder was ultimately the thermal mass and radiator surfaces of the sensor array, (2) the array cylinder mass was a portion of the sensor array mass budget and (3) the cylinder design required some provisions for thermal conduction and radiation from the sensor modules.

The final cylinder array approach was based on experience gained while working with NASA on the ARES-I Upper Stage Instrument Unit (IU). The IU was a section of primary vehicle structure upon which the payload and manned spacecraft would attach. The experience provided insight into manufacturing techniques and capabilities associated with large single piece metal forgings. Additionally, the internal volume created by the IU required thermal conditioning as it contained the majority of the flight vehicle avionics.

Current manufacturing technology allows for various methods of fabricating large diameter cylinders, whether grid stiffened or not. Each cylinder can be a set of

weldments, monocoque (single shell), skin-stringer (rivet or bolt) or a single forged item with an integral pattern machined for stiffness and weight reduction. For purposes of the case study, a single forged, non-faceted aluminum cylinder with an integral external orthogrid (arranged at right angles) pattern as shown in Figure 8 was modeled and assumed appropriate for the following reasons:

1. Ease of obtaining aluminum forgings in the design space size.

2. Aluminum is an excellent conductor and can be polished or coated for use as a radiator. Aluminum is also available in many forging sizes and thicknesses with low relative cost and consistent mechanical properties.

3. Leaving a thin "skin" for the inner diameter of the cylinder creates an ideal radiator surface.

4. A sensor module will easily integrate within square orthogrid pockets, which provide node locations for assembly as well as thermal conduction paths along the grid ribs, both vertical and circumferential. The grid pocket is also an ideal radiation path from the module to the structure "skin", which serves as the satellite radiator.

5. A single machined item has no breaks or discontinuities along potential thermal conduction paths, thus increasing the ease at which energy can be distributed throughout the cylinder.

6. A single orthogrid structure row mass can be converted to an equivalent monocoque thickness which is a variable within the thermal software utilized for the analysis.
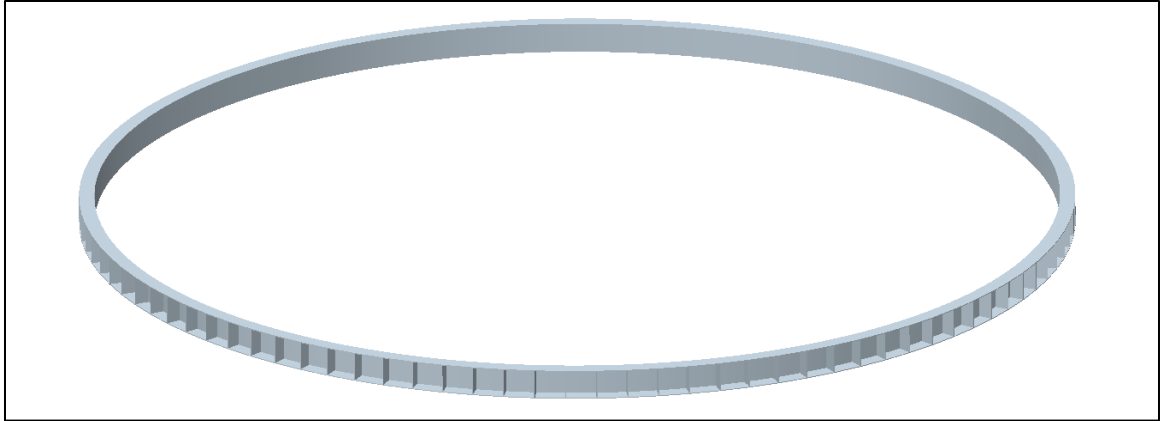
Figure 8 3D Single Row Structure Model for an Array Cylinder 3.4m in Diameter

The choice of aluminum for the structure was of concern due to the anticipated temperature swings while in orbit. Thermal distortion of the orthogrid could affect sensor alignment and position knowledge. However, if the approach was shown to satisfy the study parameters, future planners can determine if a structure which requires a minimal response to thermal expansion is required. The structural design will also become clearer as the complete sensor module design matures. A potential cylinder array structure could utilize a lower coefficient of thermal expansion composite "lattice" to constrain the sensors which then radiate heat to an inner aluminum cylinder used as a radiator.

For sizing purposes, a three-dimensional (3D) model was created with Computer Aided Manufacturing (CAD) software at 3.4 and 4.6 meters which were consistent with the maximum allowable diameters for the Taurus 2 and Falcon 9 payload fairings. A single pocket was modeled at .095 m x .095 m x .050 m, which allowed room for a .093 m x .093 m x .040 m sensor module. Each vertical and circumferential orthogrid rib was

27

modeled at minimum thicknesses achieved with computer numerical controlled (CNC) mills. Specifically, the dimensions were driven to values that can be achieved before the machining tool begins to chatter or cause "breakout." The breakout is driven by a long cutting tool required to match the pocket depth running along a tall, thin rib section. The chosen thicknesses were .003 m (0.118 inches). The inner diameter skin thickness was also modeled at .003 m (0.118 inches). Figure 9 shows a close-up of the integral machined pockets.
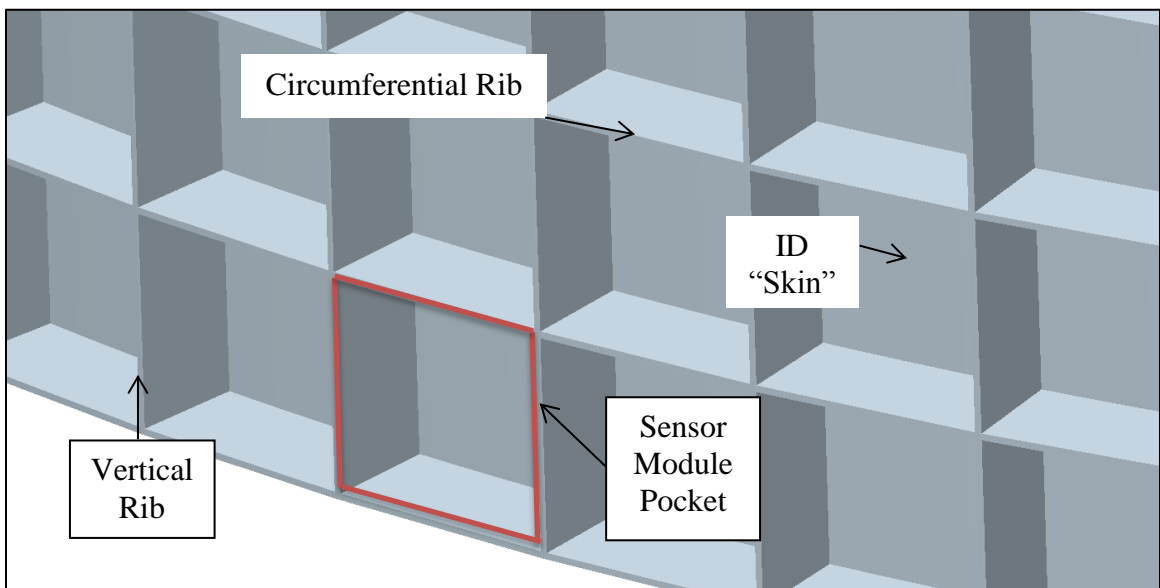
Figure 9 Machined Orthogrid Pockets

A mass was calculated for a single row of sensors at each maximum diameter. The approach allowed for the total mass to be quickly calculated by simply adding additional rows together. If a row was added, it was assumed completely filled with

sensor modules. The CAD model was also used to determine the total number of sensor module pockets available within a single row at each diameter. The resulting parameters are summarized in Table 5.

Table 5 Cylinder Mass Summary for Maximum Diameters

Parameter	3.4 m Cylinder	4.6 m Cylinder
Number of Pockets / Row	100	135
Mass / Row	21.9 kg	29.8 kg
Height / Row	.101 m	.101 m
Equivalent Thickness / Row	.0178 m (0.700 inches)	.0177 m (0.697 inches)

Additional thermal models were needed at diameters smaller than the 3.4 and 4.6 meters available. This is due to a lack of understand of the optimal spacecraft configuration which will become clearer as individual components of the system are chosen and specified.   Therefore, an identical sizing approach was utilized for cylinder diameters of 1.0 and 2.2 m. The additional diameters were chosen by the 1.2 m difference between the 3.4 m and 4.6 m arrays. The parameters are summarized in Table 6.

Table 6 Cylinder Mass Summary 1.0 m and 2.2 m

Parameter	1.0 m Cylinder	2.2 m Cylinder
Number of Pockets / Row	30	65
Mass / Row	6.1 kg	14.0 kg
Height / Row	.101 m	.101 m
Equivalent Thickness / Row	.0179 m (0.705 inches)	.0178 m (0.700 inches)

Disk

The Disk represents the spacecraft bus (dry mass) and must therefore be equal to the available mass as given in Figure 7 of 200 kg. Additionally, an accurate representation would require that any energy dissipated from the disk that impacted the sensor array was modeled. However, no internal energy output from the satellite components was modeled. Three reasons governed the assumption; (1) the component heat outputs are unknown, (2) the concern existed that the case study could become about keeping the unknown components of the disk cool as opposed to investigating passive cooling of the array and (3) the interplay of two unknown structural interfaces and conduction paths was not in scope. Therefore, the Disk was modeled as the same material of the array cylinder with a mass equal to the allocation as defined by the Ball trade study. Additionally, no conduction path was assumed between the disk and the cylinder.

Additional modeling approaches which excluded the satellite bus components were considered. One approach was a single sheet of MLI covering the opening nearest the moon as an IR shield with no assumed mass. However, including the mass representing the bus components would allow a rudimentary understanding of how the array geometry affects the disk's internal temperature. The equivalent thickness for the Disk at each diameter is as follows: .004 m (0.157 inches) at 4.6m, .008 m (0.315 inches) at 3.4 m, .019 m (0.75 inches) at 2.2 m and .092 m (3.62 inches) at 1.0 m.

MLI

A final consideration for the thermal model architecture is application of MLI. MLI is comprised of multiple layers of thin sheets separated by a small distance and coated in

thermal coatings chosen to serve a desired function. One such function is to prevent heat loss within a desired component. MLI was utilized in this thesis to reflect the sun's radiation with placement on the outside surface of the cylinder consistent with "covering" the sensor modules. Without the MLI blanket, the sensor modules would receive direct sun exposure which may lead to temperature spikes. The MLI does not prevent the desired high-energy source particles from reaching the sensors but will prevent long term build of dust on the sensor material. The MLI was also used on both surfaces of the disk to reflect radiation from both the lunar surface and the inner diameter of the cylinder. If MLI was not present in a location, the location was modeled with the same optical properties as the radiator surface.

Trial Mission Design Summary

LOCO is a cylindrical spectrometer array in lunar orbit which will utilize the moon for occultation in order to locate, identify and map deep space high-energy sources. The LOCO mission consists of individual sensor modules comprising the spectrometer array, the array cylinder on which the modules are mounted and the Disk which represents the spacecraft bus containing all components required for a functioning satellite. The system design given is based upon constraints provided by the LOCO PI. Additional effort was spent sizing the array cylinder by means of a preliminary structural design. The sizing ensured relevant constraints could be met which adds clarity and relevance to the completed thermal analysis. A description of the thermal analysis

approach for a cylindrical spectrometer array consistent with the trial science mission is

provided in the next chapter.

CHAPTER THREE

METHODOLOGY

Defined here is the thermal analysis approach for the trial science mission which brings together the elements of the background search, lunar orbit environment and passive cooling. The definition includes the analysis setup, analysis parameters, heat transfer method assumptions, reference coordinate systems, software tools, units, optical properties, thermomechanical properties, thermal model descriptions and energy inputs. The thermal description includes figures of how the thermal models are represented within the software.

Analysis Setup

Parameters

With the trial science mission architecture and constraints understood, effort could be made to define the design parameters to be varied within the thermal analysis. Parameter value selection was driven by bounding a maximum space, not specifying values

consistent with those utilized on heritage missions. The following parameters were chosen:

1. Orbit Parameters – two orbit parameters are available: orbit inclination and orbit altitude. Inclination refers to the angle of the orbit plane as rotated from the lunar equatorial place. Altitude refers to the consistent height of the circular orbit above the lunar surface. The inclination was varied to three values: 0, 75 and 90 degrees. Angles of 0 and 90 degrees close in the full orbit spectrum available while 75 degrees was provided by the LOCO PI. Altitude was also varied at two values: 10 and 1000 kilometers. The values utilized are a single order of magnitude both above and below the PI provided value of 100 km giving three values of altitudes studied.

2. Array Dimensions – two array dimensions are available: diameter and height. Diameter refers to the cylinder diameter while the height is driven by the number of sensor module rows used which is a function of total mass. The values utilized were 1.0, 2.2, 3.4 and 4.6 meters. The diameters were driven by the maximum payload fairing diameters available and linearly stepped by the difference between the two fairing sizing (1.2 m).

3. Sensor Module Energy – the energy required and dark energy created by each sensor module was PI provided. A set of analysis cases was run to determine the maximum energy which could be utilized by the sensor modules before passing the maximum array temperature limit.

Heat Transfer

With the sensor module design incomplete and a method of mounting to a structure unknown, an understanding of how heat transfers from the module to its surroundings is unknown. As with the design parameters, it was determined to run thermal models that would bound the maximum design space. Therefore, to fully investigate the passive cooling assumption, thermal models were built around two heat transfer modes:

1. Conduction Only – A conduction path exists between the sensor module and the array cylinder. The approach assumes no heat transfer by radiation.

2. Radiation Only – All heat transfer from the sensor module to the array cylinder is by radiation. The approach assumes no heat transfer by conduction.

The two assumptions chosen encompass the real world application which would involve a mix of radiative and conductive heat transfer. If neither case provided adequate cooling, then a set of thermal models would be required that utilized both heat transfer methods varied proportionately as a percentage of total heat transfer to determine if adequate cooling could be found.

For each conductive analysis, a single cylinder of an equivalent thickness detailed in Section 2 was modeled. The sensor module is assumed to conduct thermal energy to the array cylinder in a manner that the temperature of the cylinder and the sensor are identical. The only mass assumed for the cylinder was the array cylinder structural mass even though it is smaller portion of the total sensor array mass on average (~ 25%). Thermal mass from the sensor modules was not utilized. This was done for three reasons: (1) the conduction case essentially becomes removing radiation from the inside

surface of the array cylinder, (2) minimizing the mass assumed for the cylinder provides

a very conservative analysis and (3) the conductive analysis will be consistent with the

approach for the inner cylinder for the radiation case described in subsequent paragraphs.

The radiation cases consisted of two concentric cylinders of equivalent

thicknesses calculated as detailed in Section 2 and separated by a nominal distance as

shown in Figure 10.
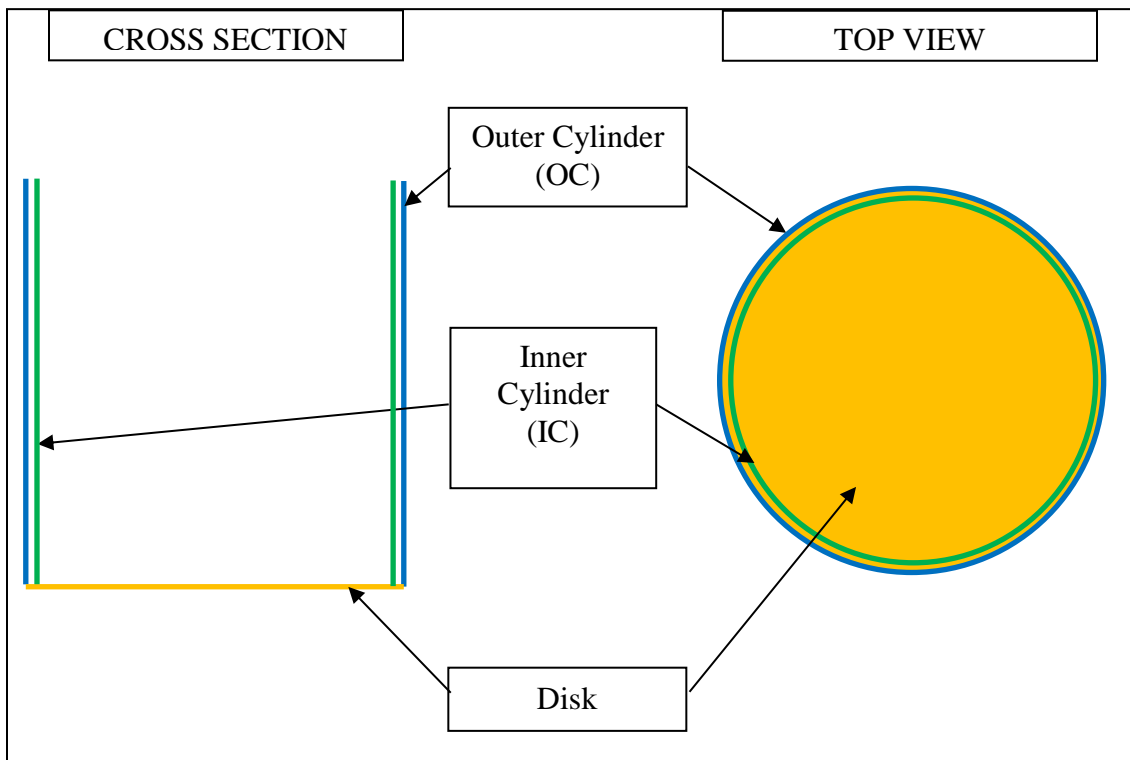
Figure 10 Radiation Case Schematic

The outer cylinder (OC) represented the sensor modules and was of diameter equivalent

to the selected analysis size. The inner cylinder (IC) represented the array structure and

was modeled with properties equivalent to the conduction case cylinders. Thermal energy moved between the two cylinders by radiation and by conduction within each individual cylinder. The surfaces between the two cylinders were modeled as radiators.

Difficulty arouse when assigning properties to the outer cylinder in the radiation models due to lack of fidelity of the sensor modules. Therefore, the outer cylinder was modeled with the mechanical properties of CsI(TI) (scintillating material) as recorded in Table 24 with a mass equivalent to the total sensor module mass for the desired case. The approach provides a conservative thermal assumption due to the low specific heat and thermal conductivity characteristics of CsI(TI).   The radiation case becomes the ability of the sensor module scintillator material to quickly radiate energy to the inner cylinder.

Approach

To fully characterize the cylindrical spectrometer array relative to each launch vehicle, a baseline analysis case was run which consisted of the constraints provided by the LOCO PI and each launch vehicle's maximum payload fairing diameter. The baseline cases were provided as a starting point and a check to determine the feasibility of passive cooling as a viable method of keeping the sensors below the maximum temperature limit. As with most studies, the importance of an individual factor may change and affect the entire outcome. For example, maximizing array diameter may not be fundamentally important. Therefore, an additional set of analyses were completed in which each specified parameter originally held constant to the PI provided values was varied. For each analysis where a parameter was changed, all others were held consistent to baseline

values in order to characterize the effect against the baseline, not a combination of parameter changes.

For each analysis case, a table will present the conductance and radiation analysis parameters and their corresponding values. The parameter values will be consistent for each heat transfer method. The parameters include the diameter, number of rows, beta angle (inclination) and altitude. The calculated cylinder height, total sensor number, total array and power utilized by the sensors, which are all a function of the number of rows selected, will be presented in the "Calculated" column. The one exception for the "Calculated" column is the sensor module power cases when the power levels are the end result of the analysis and are therefore not shown but represented by "#." Table 7 is a representation of the generic analysis case table with all parameters shown for clarity.

Table 7 Generic Analysis Case Parameter Table

Parameter	Value	Calculated
Diameter		
# of Rows		Height: Sensors: Area: Power:
Beta Angle		
Altitude		

Assumptions

1. Run Time – Each thermal model was run from an initial system temperature of 20° C until a steady state (average temperature for an orbit) was met. Additional transient orbit cases were run after reaching steady state in order to determine the maximum and minimum temperatures found during the orbit.

2. No Conduction between Cylinder and Disk – No conduction paths were modeled between the Disk and the cylinder. This was based on the assumption that the power dissipated within the satellite components would be needed to maintain nominal operating temperatures within control electronics and propulsion systems. Therefore the bus would be thermally isolated from the cylinder and only affect the cylinder through radiation. Radiation still occurred normally between cylinder and the MLI covering the Disk.

3. Orbit Positions Analyzed – Each orbit was divided into 20 degree increments.

4. No Heat Load within Disk – No heat load was applied to the disk even though it would be required for avionics and keeping components warm. This decision was justified by a case completed to determine the effect of a Disk central heat load. The heat load was found to increase the temperature of the Disk to a higher steady state point but to not affect the cylinder in any appreciable way, which is consistent with no conduction paths.

Analysis Cases

The final component in each analysis case is to determine the number of sensors. The number of sensors drives the total mass, array area and energy required. The number of sensors per case was determined by creating a total mass number for an individual row at the chosen array diameter. The structural mass and number of sensors available per row for a given diameter was provided earlier in Table 5 and Table 6. The total row mass was created by adding the total sensor module mass for a given diameter to the structural row mass. Rows were then added until the payload capacity for the given launch vehicle was reached without being eclipsed as depicted in Figure 11.
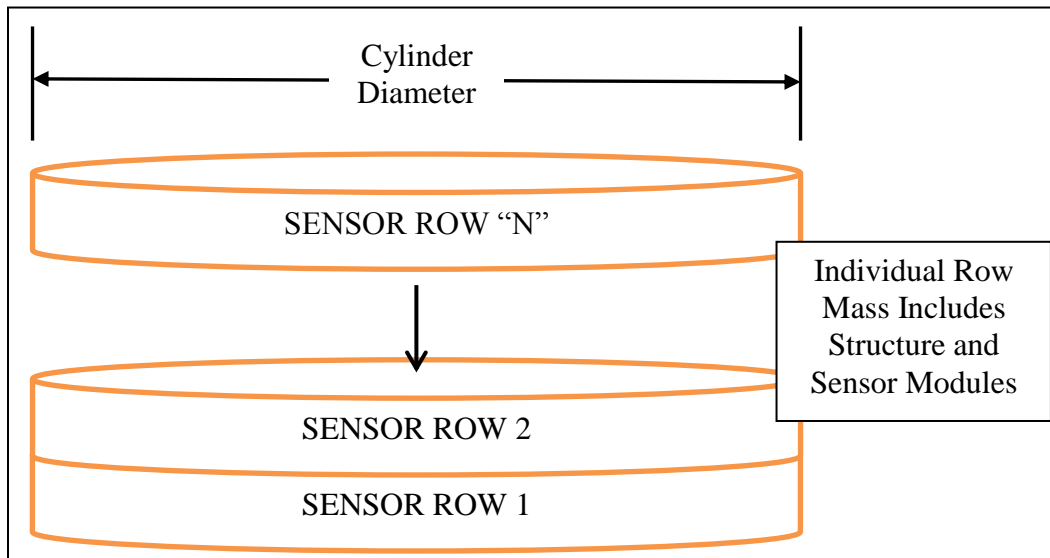
Figure 11 Array Mass Calculation from Individual Rows

Table 8 summarizes the total mass for a given number of rows and array diameter.

Table 8 Total Row Mass (kg) Per Cylinder Diameter

ROWS	1.0 m	2.2 m	3.4 m	4.6 m
1	32.1	70.4	108.7	147.0
2	64.3	140.8	217.4	294.0
3	96.4	211.3	326.1	440.9
4	128.6	281.7	434.8	587.9
5	160.7	352.1	543.5	734.9
6	192.8	422.5	652.2	881.9
7	225.0	492.9	760.9	1028.9
8	257.1	563.4	869.6	1175.8
9	289.3	633.8	978.3	1322.8
10	321.4	704.2	1087.0	1469.8
11	353.5	774.6	1195.7	1616.8
12	385.7	845.0	1304.4	1763.8
13	417.8	915.5	1413.1	1910.7
14	450.0	985.9	1521.8	2057.7
15	482.1	1056.3	1630.5	2204.7
16	514.2	1126.7	1739.2	2351.7
30	964.2	2112.6	3261.0	4409.4
31	996.3	2183.0	3369.7	4556.4
32	1028.5	2253.4	3478.4	4703.4

As an example, Table 5 shows that a 3.4m row structural mass is 21.9 kg and permits the usage of 100 sensors. The total sensor module mass is found by multiplying the 100 sensors with the individual sensor mass of .868 kg (Table 3) for a total of 86.8 kg. When combined with the structural mass, a final total mass per row is 108.7 kg. The launch capacity of the Taurus 2 is 490 kg (Figure 7) which would allow for 4 rows of sensors before being eclipsed. This would preclude the desired total array viewing area of 4 m^2. The desired area can be easily achieved on the Falcon 9, yet the analysis cases

are presented in such a way as to show what can be accomplished against each baseline as shown in Figure 12.
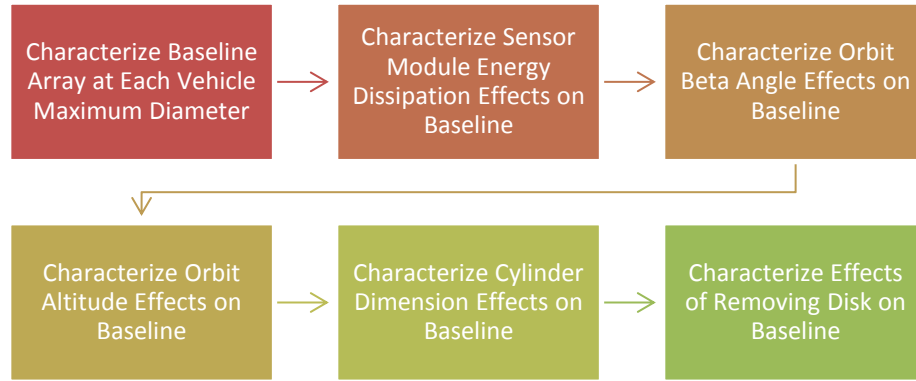
Figure 12 Analysis Cases Progression Summary

Baseline

The Falcon 9 mass limit of 895 kg (Figure 7) was used as the driver for the 4.6 m diameter array. Using Table 8 it was determined that 6 rows could be utilized and remain within the mass limit. The Taurus 2 mass limit of 490 kg (Figure 7) was used as the driver for the 3.4 m diameter array. Using Table 8 it was determined that 4 rows could be utilized within the mass limit. The conductance and radiation baseline cases for the 4.6 m and 3.4 m diameter cylinders are presented in Table 9 and Table 10.

Table 9 Baseline Conduction and Radiation Cases – 4.6 m

Parameter	Value	Calculated
Diameter	4.6 m	
# of Rows	6	Height: 0.606 m Sensors: 810 Area: 5.16 m^2 Power: 69.7 Watts
Beta Angle	75°	
Altitude	100 km, Circular Orbit	

Table 10 Baseline Conduction and Radiation Cases – 3.4 m

Parameter	Value	Calculated
Diameter	3.4 m	
# of Rows	4	Height: 0.404 m Sensors: 400 Area: 2.55 m^2 Power: 34.4 Watts
Beta Angle	75°	
Altitude	100 km, Circular Orbit	

Sensor Module Energy Cases

Consistent with Assumption 4, the satellite components which are spatially represented by the Disk do not provide any thermal load to the array cylinder except through radiation. To provide some insight into the effects of a larger power level dissipated by the sensor modules, the total module wattage was increased until the array maximum temperature limit was exceeded. The conductance and radiation energy cases are presented in Table 11 and Table 12.

Table 11 Sensor Module Energy Conduction and Radiation Analysis Cases – 4.6 m

Parameter	Value	Calculated
Diameter	4.6 m	
# of Rows	6	Height: 0.606 m Sensors: 810 Area: 5.16 m^2 Power: #
Beta Angle	75°	
Altitude	100 km, Circular Orbit	

Table 12 Sensor Module Energy Conduction and Radiation Analysis Cases – 3.4 m

Parameter	Value	Calculated
Diameter	3.4 m	
# of Rows	4	Height: 0.404 m Sensors: 400 Area: 2.55 m^2 Power: #
Beta Angle	75°	
Altitude	100 km, Circular Orbit	

Orbit Cases

The orbit parameters available within the circular orbit needed for occultation are the

altitude and beta angle. The altitudes considered were 10 and 1000 km which are an

order of magnitude both below and above the baseline value. The beta angles

(inclination) considered were 0°degrees (equatorial) and 90 degrees (polar) which

enveloped the available angles. The conductance and radiation orbit cases are presented

in Table 13 through Table 16.

Table 13 Orbit Beta Angle Conduction and Radiation Cases – 4.6 m

Parameter	Value	Calculated
Diameter	4.6 m	
# of Rows	6	Height: 0.606 m Sensors: 810 Area: 5.16 m^2 Power: 70 Watts
Beta Angle	0° (Equatorial) & 90°	
Altitude	100 km, Circular Orbit	

Table 14 Orbit Altitude Conduction and Radiation Cases – 4.6 m

Parameter	Value	Calculated
Diameter	4.6 m	
# of Rows	6	Height: 0.606 m Sensors: 810 Area: 5.16 m^2 Power: 70 Watts
Beta Angle	75°	
Altitude	10 & 1000 km, Circular Orbit	

Table 15 Orbit Beta Angle Conduction and Radiation Cases – 3.4 m

Parameter	Value	Calculated
Diameter	3.4 m	
# of Rows	4	Height: 0.404 m Sensors: 400 Area: 2.55 m^2 Power: 34 Watts
Beta Angle	0° (Equatorial) & 90°	
Altitude	100 km, Circular Orbit	

Table 16 Orbit Altitude Conduction and Radiation Cases – 3.4 m

Parameter	Value	Calculated
Diameter	3.4 m	
# of Rows	4	Height: 0.404 m Sensors: 400 Area: 2.55 m^2 Power: 34 Watts
Beta Angle	75°	
Altitude	10 & 1000 km, Circular Orbit	

Dimension Cases

The mass budget used throughout the analysis is based on preliminary findings and assumptions affecting each case when a large cylinder diameter is the primary driver. Therefore, a set of cases was completed where the maximum diameter was not the driver. The larger mass allocation of the Falcon 9 (895 kg) was chosen and consideration was given to exceeding the mass allocation by 10% (90 kg) for a total of 985 kg. The 10% was applied by removing some of the margin within the Ball Aerospace trade study. The Falcon 9 mass was chosen to be utilized for each diameter thus bounding the capabilities of the Taurus 2. For each decrease in diameter, the height and consequently sensor area were increased until the new mass limited was reached without being eclipsed.

Using Table 8 and the increased mass allocation limit of 985 kg, it was determined that the number of rows for the 4.6 m cylinder could not increase and no new analysis was completed. For the 3.4, 2.2 and 1.0 m diameter cylinders the number of rows used were 9, 14 and 30 respectively. The conductance and radiation dimension cases are presented in Table 17 through Table 19.

Table 17 Dimension Conduction and Radiation Cases – 3.4 m

Parameter	Value	Calculated
Diameter	3.4 m	
# of Rows	9	Height: 0.909 m Sensors: 900 Area: 5.73 m^2 Power: 77.4 Watts
Beta Angle	75°	
Altitude	100 km, Circular Orbit	

Table 18 Dimension Conduction and Radiation Cases – 2.2 m

Parameter	Value	Calculated
Diameter	2.2 m	
# of Rows	14	Height: 1.414 m Sensors: 910 Area: 5.80 m^2 Power: 78.3 Watts
Beta Angle	75°	
Altitude	100 km, Circular Orbit	

Table 19 Dimension Conduction and Radiation Cases – 1.0 m

Parameter	Value	Calculated
Diameter	1.0 m	
# of Rows	30	Height: 3.030 m Sensors: 900 Area: 5.73 m^2 Power: 77.4 Watts
Beta Angle	75°	
Altitude	100 km, Circular Orbit	

No Disk Cases

A final set of cases were run after a review of the results of the previous cases. The new

analyses removed the Disk from the model architecture. The "No Disk" cases are not

considered a viable approach as a satellite bus is a required element for an operating

spacecraft. The cases were run for data and to provide insight into the issues associated

with thermal control in a lunar orbit due to the addition of lunar IR. The selected cases

were the 4.6 baseline conduction and radiation cases as well as the 1.0 conduction and

radiation cases. The conductance and radiation No Disk cases are presented in Table 20.

Table 20 No Disk Cases – 4.6 m

Parameter	Value	Calculated
Diameter	4.6 m	
# of Rows	6	Height: 0.606 m Sensors: 810 Area: 5.16 m^2 Power: 69.7 Watts
Beta Angle	75°	
Altitude	100 km, Circular Orbit	

Table 21 No Disk Cases – 1.0 m

Parameter	Value	Calculated
Diameter	1.0 m	
# of Rows	30	Height: 3.030 m Sensors: 900 Area: 5.73 m^2 Power: 77.4 Watts
Beta Angle	75°	
Altitude	100 km, Circular Orbit	

Models

Thermal Desktop® allows the user to input the planet and orbit type, model geometry and thickness, insulation location, material properties and heat loads among other parameters. The following section describes the thermal model coordinate system, inputs, units, optical properties, thermomechanical properties and visual depictions created within Thermal Desktop®. The section also discloses the additional software used for mechanical modeling and data reduction.

In order to draw confidence in the results from the computer thermal models, hand calculations were completed. The calculations compared the total energy absorbed by LOCO to the total energy which could be emitted based upon available radiator surface area. The total energy absorbed was a function of the orientation of the array in relation to the sun, mass and material properties. The energy emitted was a function of radiator surface area, material properties and view factors due to the cylindrical geometry. If the total energy absorbed remained at or below the energy which could be emitted, it was concluded that the array temperatures could be maintained as desired. This approach was utilized as the calculations assumed the array was always in view of the sun in order to add conservatism.

Tools

Thermal models of the LOCO array were created and analyzed using Cullimore and Ring Technologies' Thermal Desktop® (www.crtech.com). Preliminary structural models for

mass assumptions were created in Parametric Technology Corporation's Pro/Engineering Wildfire 5©. Data was reduced and plotted using Microsoft Excel and Thermal Desktop.

Reference Coordinate Systems

The co-planer alignment of the equators of the sun and the moon used in the thermal models is depicted in Figure 13. Also depicted is the Beta Angle which is defined as the angle created by the rotation about the -Y Lunar Axis of the satellite orbit plane from the lunar equatorial plane. The cylinder array reference coordinate system is depicted in Figure 14.

1. Lunar Coordinate System

    a. X-Axis: +X oriented toward the solar vector.

    b. Z-Axis: +Z oriented toward the North Lunar Pole.

    c. X-Y Plane: Plane along which the sun and lunar equator lies.

    d. Beta Angle: Rotation of X-Y Plane about the -Y Axis
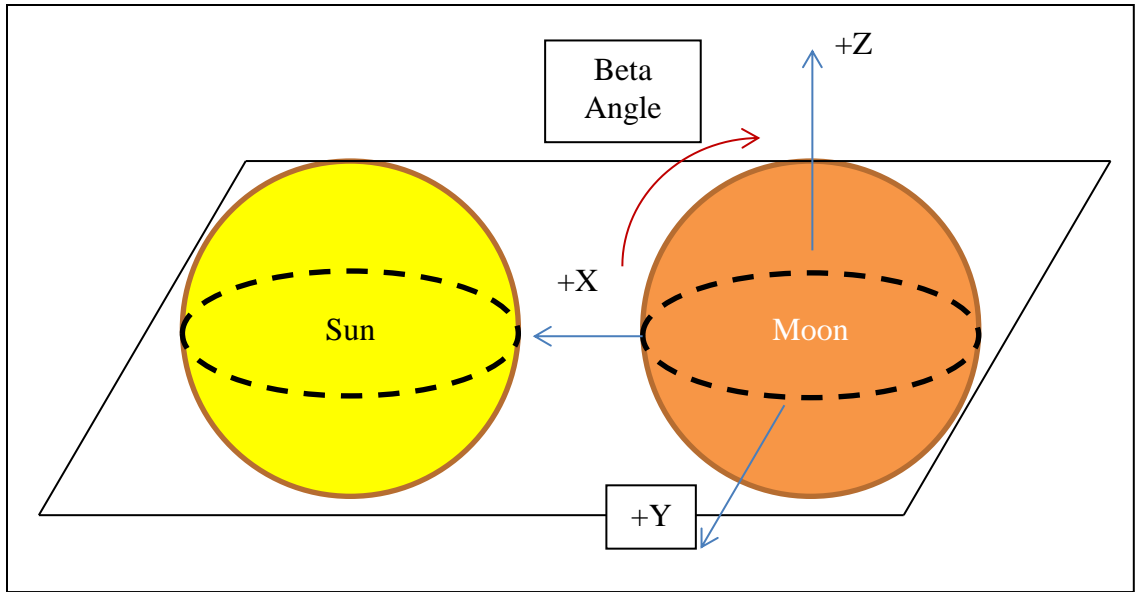
Figure 13 Orientation of Sun in Relation to Moon

2. Array Coordinate System

   a. X-Axis: +X oriented along counter clock wise (CCW) direction of
      orbit plane viewed from Lunar North Pole (velocity vector).

   b. Y-Axis: +Y oriented towards Lunar North Pole at equatorial orbit.

   c. Z-Axis: +Z oriented along Nadir through the geometric center of the
      moon.

   d. X-Z Plane: Orbit plane.
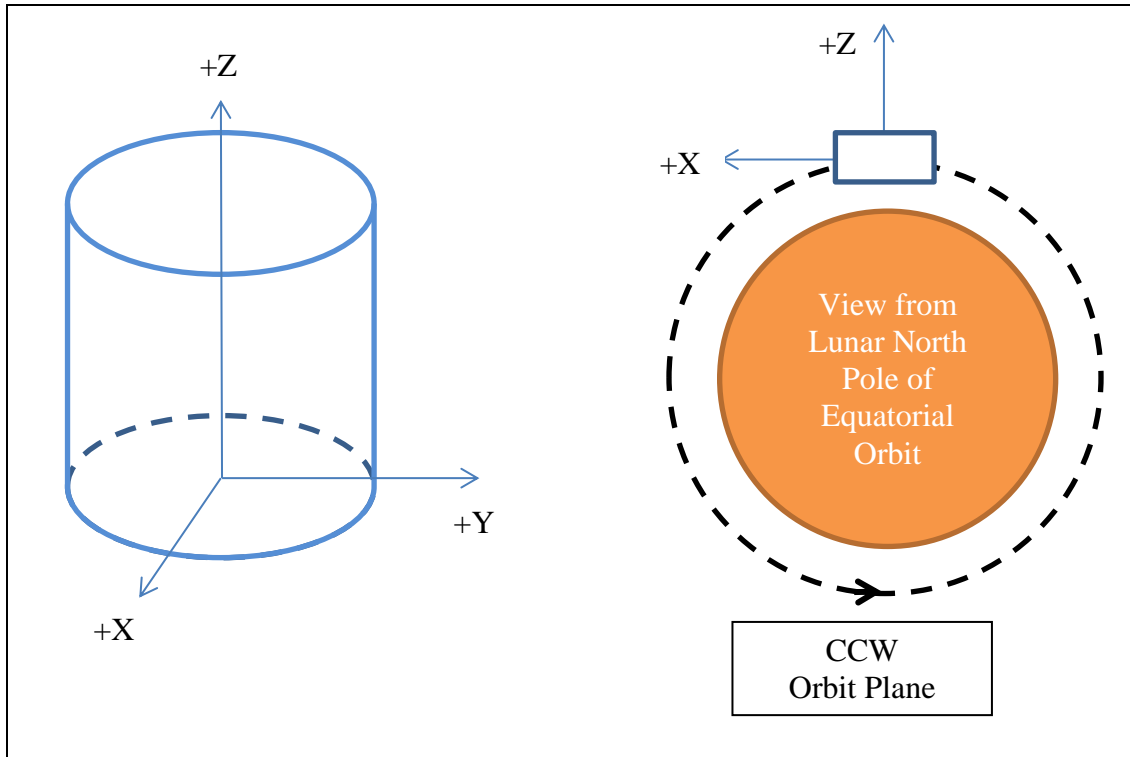
Figure 14 Array Coordinate System

Units

The following units were used for the performed analyses and are depicted in Table 22.

Table 22 Units Summary

Parameter	Unit
Time	Seconds (s)
Length	Meters (m) / Kilometers (km)
Power	Watts (W)
Temperature	Celsius (°C)
Energy	Joules (J)
Mass	Grams (g) / Kilograms (kg)

Optical Properties

All MLI and radiator surface coatings were chosen to maximize values of absorptivity and emissivity for a given purpose. In the case of the MLI outer layer, minimum values for absorptivity and emissivity aim to reduce the solar energy and lunar IR that reaches the sensor array. Radiator coatings desire high emissivity values for maximum rejected radiation and low absorptivity values to minimize solar flux input. The optical properties of the materials chosen are summarized in Table 23.

Table 23 Optical Properties Summary

Material	Usage	Absorptivity	Emissivity	Source
Aluminized Kapton	MLI Outer Layer	0.23	0.24	Spacecraft Thermal Control Handbook (Henniger 2002)
Aluminized Kapton	MLI Insulation and Core	Effective Emissivity: 0.01		
Magnesium Oxide / Aluminum Oxide Paint	Radiator Surface	0.09	0.92	

Thermomechanical Properties

The thermomechanical properties of the MLI, aluminum and scintillating material (CSI(Ti)) used are summarized in Table 24.

Table 24 Thermomechanical Properties

Material	Property	Value	Source
Aluminum	Specific Heat	864 J/kg-C	MatWeb (MatWeb 2012)
	Thermal Conductivity	120 W/m-C	
	Density	2840 kg/m^3	
MLI	Effective Emissivity	.01	Spacecraft Thermal Control Handbook (Henniger 2002)
	Maximum Temperature	250 C Continuous	
	Minimum Temperature	-250 C Continuous	
CSI(Ti)	Specific Heat	0.048 J/kg-C	Hilger Crystals (Properties of CsI(Tl) 2010)
	Thermal Conductivity	1.13 W/m-C	
	Density	4510 kg/m^3	

Model Features

1. Nodes – The nodes are point locations at which data is provided and are depicted by small spheres. Each model was broken into 20 degree segments centered from the middle of the disk. The disk was divided radially an additional 4 times while each cylinder was divided by one more than the number of rows needed to generate the required sensor area to ensure a node at each end (10 divisions for 9 rows for example). Cylinder wall thickness was a model parameter and was thin enough to be captured by a single layer of nodes as depicted in Figure 14 (array of node "columns"). The disk and cylinder share coincident node locations.

2. Sensor Module Power – The sensor module power is modeled as red arrows and depicts a uniform, continuous input equal to the number of sensor modules multiplied by their corresponding energy input. The sensor module power is always applied at the cylinder where the sensor modules are located.

3. Division Lines – Show the sections about which the model has been divided for node locations.

Figure 15 depicts a full conduction thermal model as viewed within Thermal Desktop® and is provided to show common model features.
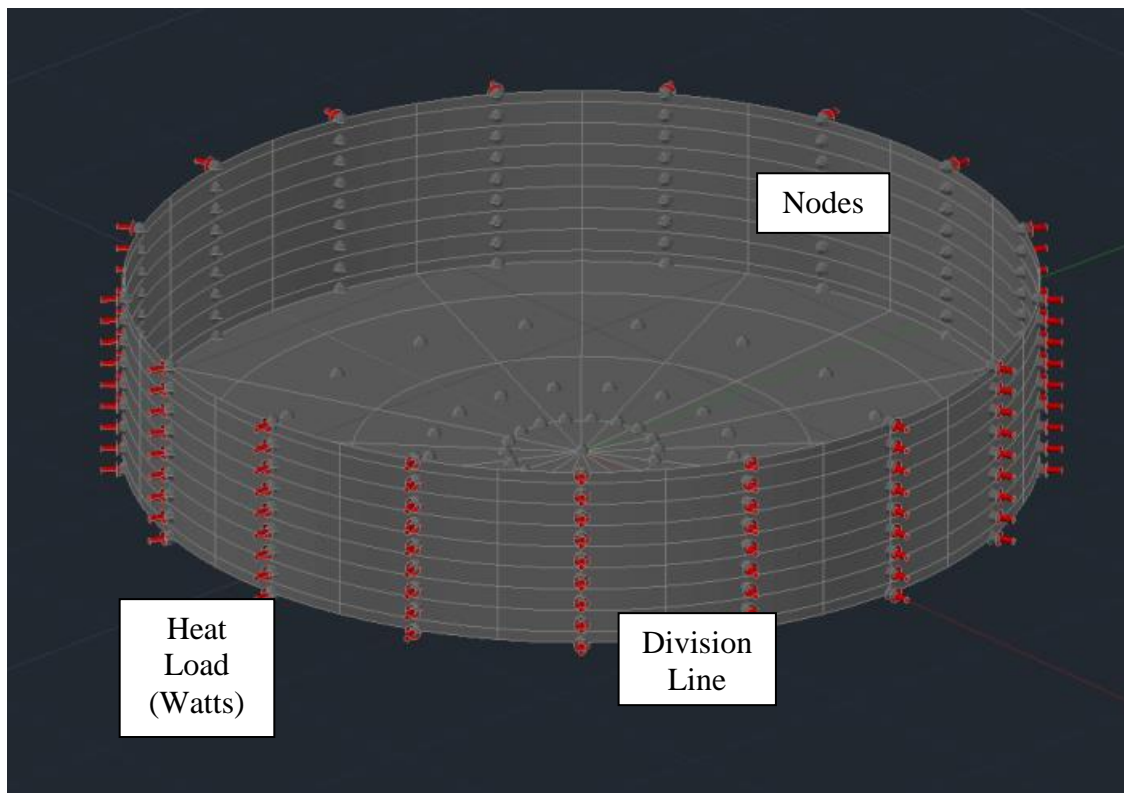
Figure 15 Thermal Model Features

Model Depictions

Two thermal models were created to analyze the full conduction and full radiation cases.

Figure 16 and Figure 17 show a view of a conductive array cylinder from an isometric

perspective at the top and the bottom.
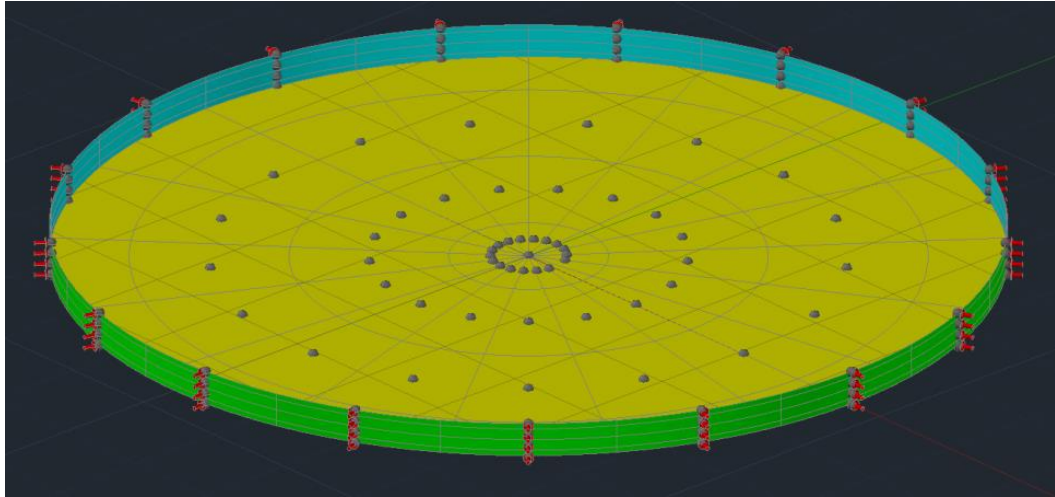
Figure 16 Model Surfaces Viewed from Top
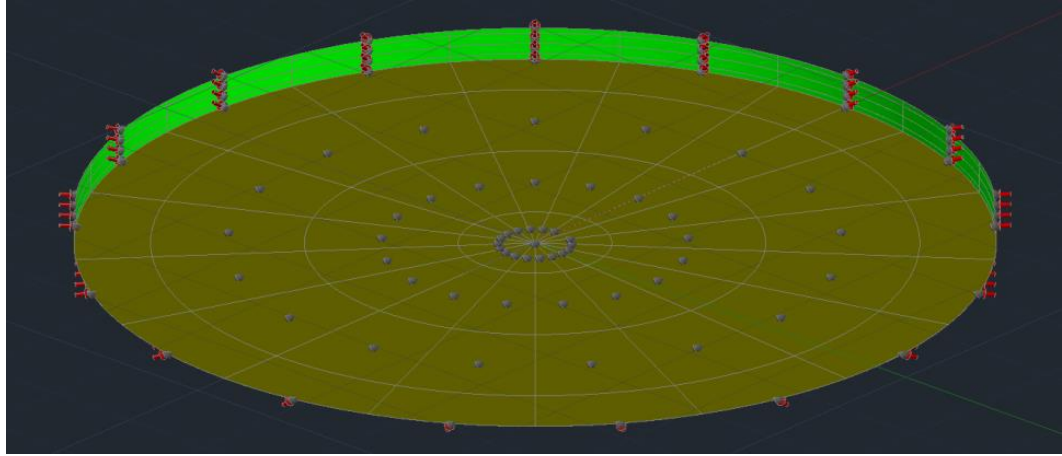
Figure 17 Model Surfaces Viewed from Bottom

Figure 18 is a close-up of the full radiation thermal model as viewed within Thermal Desktop. The close-up is provided to show the small gap between the two cylinders needed for the radiation case.
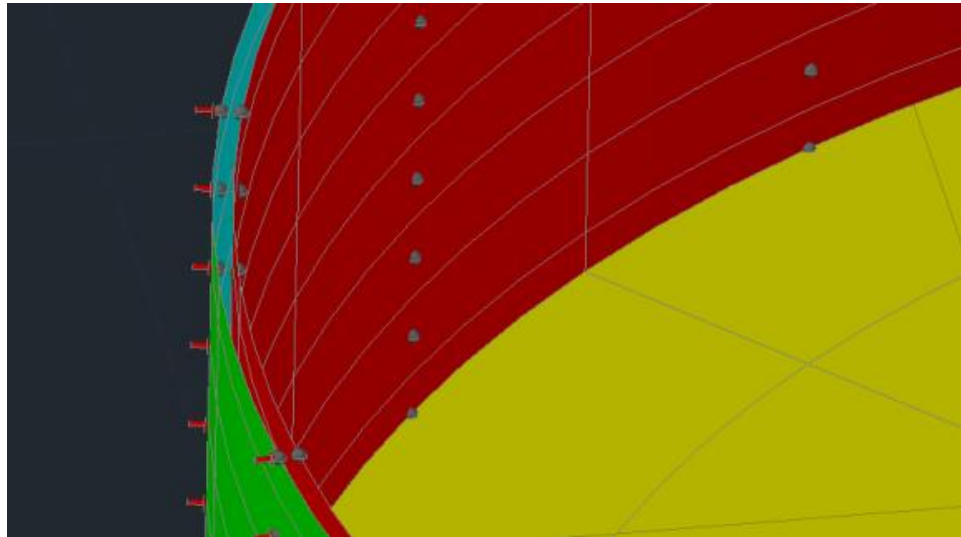
Figure 18 Close-Up of Radiation Model

Figure 19 depicts an equatorial orbit with sun shadow in a purple grid. The sensor array is enlarged for clarity. The red surface color depicts the surface temperature which is greater on the side of the moon facing the sun.
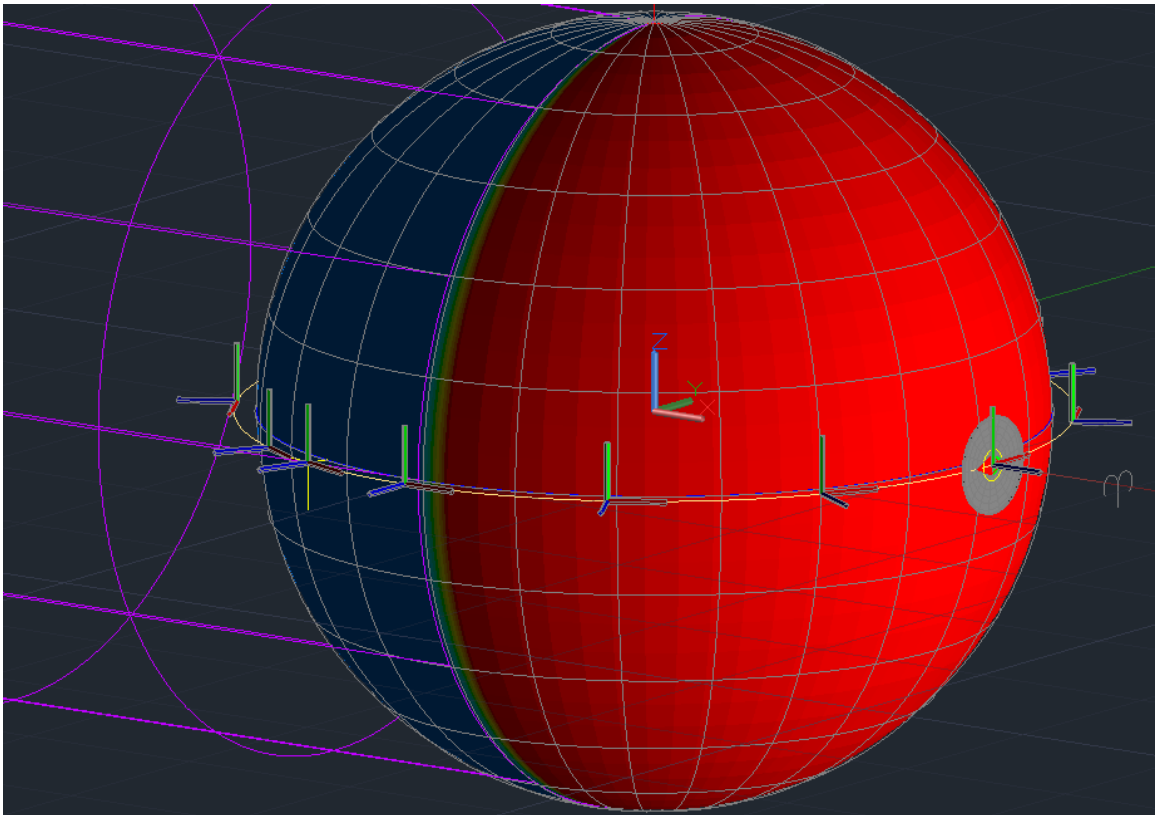
Figure 19 Model Orbit Example and Coordinate Systems

Thermal Load Sources

The thermal loads modeled are depicted in Table 25 and Figure 20. The Sun's rays are assumed collimated when they reach the satellite and moon. The angle of incidence

between the sun's rays and each irradiated surface changes as the satellite and moon maintain their respective orbits.

Table 25 Thermal Load Sources

Load	Value	Source
(1) Sensor Module	.086 Watts Continuous	Dr. Richard Miller (R. S. Miller, private communication 2011)
(2) Solar Radiation (Irradiance)	Mean value exposure of 1354 W/m^2 throughout the exposed satellite orbit	Spacecraft Thermal Control Handbook (Henniger 2002)
(3) Lunar Albedo (diffuse)	Mean value of 0.1	
(4) Lunar IR (Infrared)	Surface temperature of 119 °C on the sun side and -105 °C on the dark side	
(5) Satellite Bus Waste Radiation (Disk to Cylinder)	Waste radiation was driven by the analysis geometry which drove radiation paths	Determined by thermal model during each run case
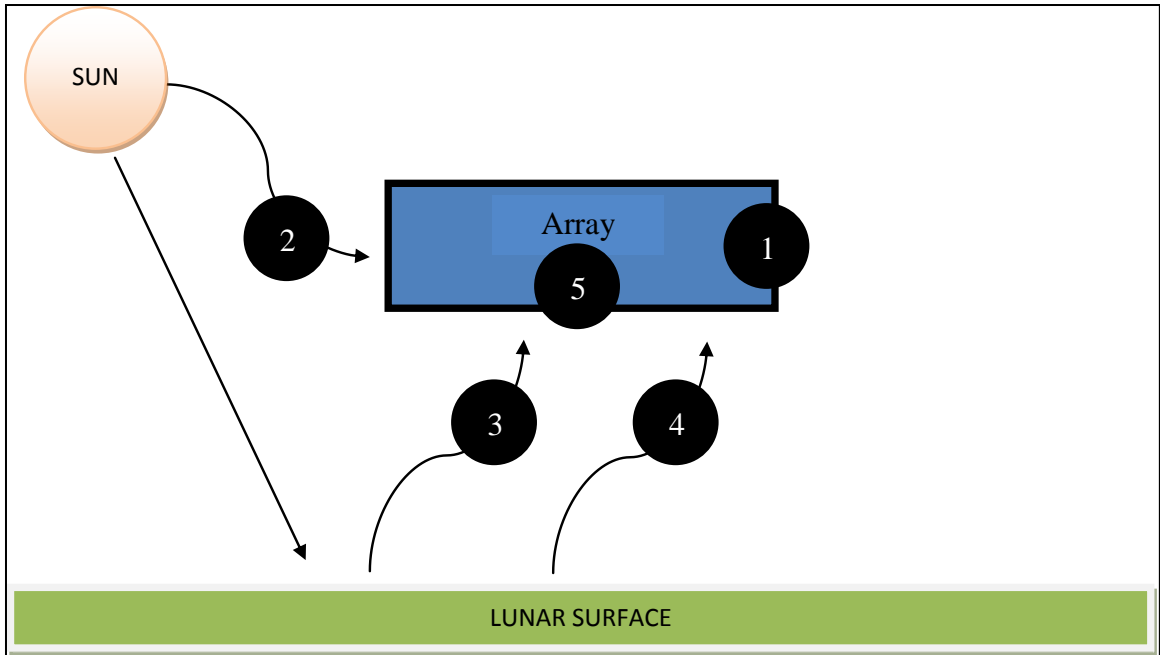
Figure 20 Thermal Load Map

CHAPTER FOUR

RESULTS AND CONCLUSIONS

Presented here are the results from the thermal analysis. The results are summarized in table format and are followed by a discussion of the conclusions for each case type when compared to the baseline results. A summary of the analysis approach is found at the end of the chapter along with general conclusions.

Results

MLI temperatures will not appear in the results as they did not exceed 150° C on any MLI surface thus remaining below safe usage temperatures. Analysis results are tabulated under the following column categories unless otherwise specified:

- Maximum – Highest single node temperature found during the analysis

- Minimum – Lowest single node temperature found during the analysis

- Delta – The largest temperature swing found for a single node during a full orbit. This value should not be confused with the difference between the highest and lowest single node temperatures found.

- Disk – The highest single node temperature found for the Disk

Baseline Case Results

Table 26 Baseline Results – 4.6 m

Case	Max (°C)	Min (°C)	Delta (°C)	Disk (°C)
Conductance	-54.3	-111.3	18.2	23.5
Radiation – Outer Diameter	-46.7	-103.2	20.2	22.8
Radiation – Inner Diameter	-53.4	-113.7	18.3	

Table 27 Baseline Results – 3.4 m

Case	Max (°C)	Min (°C)	Delta (°C)	Disk (°C)
Conductance	-57.0	-110.2	18.1	20.6
Radiation – Outer Diameter	-49.4	-100.2	21.2	20.1
Radiation – Inner Diameter	-56.5	-111.8	18.6	

The baseline analysis cases which are driven by maximizing usage of the available

fairing diameters and the LOCO constraints demonstrate that a passive cooling approach

is valid. The Disk did not see any appreciable temperature change compared to its initial

temperature. As a reminder, the Disk is isolated from the Cylinder and has no internal

energy supply consistent with Assumptions 2 and 4 found earlier in the thesis.

62

Sensor Module Energy Case Results

The maximum node temperature for each case is equivalent to the maximum temperature allowable of 0° C and was therefore not recorded. The maximum wattage used to exceed the sensor temperature allowable is substituted for maximum temperatures in the results tables. As a reminder, the sensor wattage was increased in the array until the maximum temperature limit was exceeded.

Table 28 Energy Case Results – 4.6 m

Case	Max Wattage	Min (°C)	Delta (°C)	Disk (°C)
Conductance	1100	-28.5	17.9	26.6
Radiation – Outer Diameter	600	-33.0	16.0	24.5
Radiation – Inner Diameter	N/A	-60.9	18.2	

Table 29 Energy Case Results – 3.4 m

Case	Max Wattage	Min (°C)	Delta (°C)	Disk (°C)
Conductance	550	-28.7	18.0	23.4
Radiation – Outer Diameter	300	-32.2	16.7	21.6
Radiation – Inner Diameter	N/A	-60.8	18.8	

The energy case results demonstrate that the under the constraints of the analysis, the

spectrometer array can utilize more power compared to the baseline power usage without

driving array temperatures above limit. An acceptable increase of nearly 16 times the

baseline power was found for the conductance and over 8.5 times for the radiation cases

on average. The 4.6 and 3.4 m cases behave in almost the same manner. The Disk did

not see any appreciable temperature change compared to its initial temperature.

Orbit Analysis Case Results

Orbit case results are grouped by beta angle and altitude to make commenting on the

results more clear to the reader as the 4.6 and 3.4 m cases behave in the same manner.

Table 30 Orbit Beta Angle 0° Results – 4.6 m

Case	Max (°C)	Min (°C)	Delta (°C)	Disk (°C)
Conductance	-45.7	-74.2	20.3	44.9
Radiation – Outer Diameter	-29.1	-70.3	37.6	42.4
Radiation – Inner Diameter	-46.5	-73.5	21.4	

Table 31 Orbit Beta Angle 90° Results – 4.6 m

Case	Max (°C)	Min (°C)	Delta (°C)	Disk (°C)
Conductance	-119.4	-135.3	2.7	1
Radiation – Outer Diameter	-93.4	-123.5	2.1	0.9
Radiation – Inner Diameter	-102.3	-137.0	2.7	

Table 32 Orbit Beta Angle 0° Results – 3.4 m

Case	Max (°C)	Min (°C)	Delta (°C)	Disk (°C)
Conductance	-47.7	-74.0	19.7	43.6
Radiation – Outer Diameter	-29.7	-69.3	37.3	41.2
Radiation – Inner Diameter	-46.5	-72.5	21.4	

Table 33 Orbit Beta Angle 90° Results – 3.4 m

Case	Max (°C)	Min (°C)	Delta (°C)	Disk (°C)
Conductance	-121.7	-134.4	2.1	0.8
Radiation – Outer Diameter	-95.8	-123.2	1.9	0.7
Radiation – Inner Diameter	-123.9	-136.2	2.1	

The 0° cases provide three interesting results: (1) the Disk temperature is nearly doubled,

(2) the minimum temperatures were warmer in general and (3) the outer diameter

warmed significantly while experiencing larger temperatures swings during each orbit.

The 90° cases were much colder than the baseline case temperatures cutting the Disk

temperature in half while minimizing the temperature swings relative to a single node.

Table 34 Orbit Altitude 10 km Results – 4.6 m

Case	Max (°C)	Min (°C)	Delta (°C)	Disk (°C)
Conductance	-54.2	-114.5	16.8	20.9
Radiation – Outer Diameter	-45.5	-108.4	21.1	19.4
Radiation – Inner Diameter	-53.1	-116.8	17.2	

Table 35 Orbit Altitude 1000 km Results – 4.6 m

Case	Max (°C)	Min (°C)	Delta (°C)	Disk (°C)
Conductance	-49.6	-115.1	30.9	-13.4
Radiation – Outer Diameter	-43.9	-106.4	30.9	-14.2
Radiation – Inner Diameter	-48.4	-117.4	31.6	

Table 36 Orbit Altitude 10 km Results – 3.4 m

Case	Max (°C)	Min (°C)	Delta (°C)	Disk (°C)
Conductance	-56.8	-114.2	16.8	18
Radiation – Outer Diameter	-49.0	-107.5	21.0	16.5
Radiation – Inner Diameter	-56.7	-115.5	17.5	

Table 37 Orbit Altitude 1000 km Results – 3.4 m

Case	Max (°C)	Min (°C)	Delta (°C)	Disk (°C)
Conductance	-52.0	-113.6	32.1	-16.4
Radiation – Outer Diameter	-46.7	-103.5	32.1	-17.1
Radiation – Inner Diameter	-51.4	-115.3	32.7	

The altitude case results demonstrated that moving closer to the lunar surface did not result in changes more than a few degrees compared to the baseline. The trend was similar in moving from the lunar surface save for an increased temperature swing during each orbit. Of particular interest is the Disk temperature for the radiation cases at higher altitude in that it cooled nearly 2 times below its original baseline temperature of 20° C.

Cylinder Dimension Case Results

Table 38 Dimension Results – 3.4 m

Case	Max (°C)	Min (°C)	Delta (°C)	Disk (°C)
Conductance	-73.1	-102.4	12.5	19
Radiation – Outer Diameter	-67.9	-96.2	14.2	18.4
Radiation – Inner Diameter	-73.6	-103.4	12.8	

Table 39 Dimension Results – 2.2 m

Case	Max (°C)	Min (°C)	Delta (°C)	Disk (°C)
Conductance	-76.5	-87.9	9.2	19.5
Radiation – Outer Diameter	-65.8	-88.9	12.8	18.9
Radiation – Inner Diameter	-75.5	-88.8	10.9	

Table 40 Dimension Results – 1.0 m

Case	Max (°C)	Min (°C)	Delta (°C)	Disk (°C)
Conductance	-9.4	-42.0	6.7	33.8
Radiation – Outer Diameter	-0.9	-43.0	8.6	34.3
Radiation – Inner Diameter	-6.7	-43.0	6.8	

The dimension case results are of particular interest due to their similarity in the number of sensors, sensor area and power utilized as shown in Table 17 through Table 19. The results demonstrated that a gain in cylinder height at the expense of diameter could decrease overall node temperature as well as temperature swings during a full orbit when compared to the baseline. However, as the height continues to increase there will come a point (as seen in the 1.0 m array) that the temperature swing will continue to decrease while increasing the temperature of the sensors and the Disk almost to the point of passing the given limits.

No Disk Case Results

Table 41 No Disk Results – 4.6 m

Case	Max (°C)	Min (°C)	Delta (°C)	Disk (°C)
Conductance	27.3	-30.6	30.7	
Radiation – Outer Diameter	39.6	-33.6	42.7	N/A
Radiation – Inner Diameter	30.6	-38.7	31.8	

Table 42 No Disk Results – 1.0 m

Case	Max (°C)	Min (°C)	Delta (°C)	Disk (°C)
Conductance	54.7	-16.9	27.8	
Radiation – Outer Diameter	61.7	-22.1	37.4	N/A
Radiation – Inner Diameter	57.5	-20.5	29.9	

In both No Disk cases, the maximum array temperature limit was exceeded. As a reminder the removal of the Disk allows the lunar IR to reach the surface of the radiator.

Conclusions

This thesis evaluated a passively cooled cylindrical spectrometer array in lunar orbit. The evaluation demonstrated that the passive cooling approach allowed the maintenance of the spectrometer array below a desired maximum operating temperature. A background search of historical lunar missions was provided giving perspective on thermal issues and controls of space science instruments. Next, a trial science mission was designed and analyzed which brought together the elements of the background search, lunar orbit environment and passive cooling. Finally, the trial science mission analysis results were provided along with conclusions drawn about each analysis case.

The analysis results clearly show that the sensor array cylinder can remain below the maximum temperature limit with passive means and without adding any additional radiator surfaces to the cylinder. The analysis also showed that array temperature could be kept below the maximum by either keeping a large diameter and minimizing height, or

decreasing the diameter while increasing the height. This observation allows great lee

way for future decision-makers.

Meeting the desired sensor array surface area required the capabilities of the

Falcon 9 vehicle and an emphasis on a smaller diameter driving a greater cylinder height.

Individual sensors did not see temperature swings greater than 40° C save for the 4.6 m

"No Disk Radiation" case. From a systems perspective viewing the array as a whole,

each array had a typical temperature swing of 50 to 60° C. Future considerations include:

1. Isolating the inner radiating surface of the cylinder from the lunar IR is critical to
   maintaining temperatures below the maximum allowable.

2. Disk temperature did not see dramatic changes from its initial regardless of the
   analysis case. Therefore, heat generated within the spacecraft bus may cause high
   temperature issues unless a need for heating systems to support a subsystem
   (propulsion) is demonstrated.

3. The cylindrical configuration appears to be very tolerant to change in dimensions
   and large swing in power required for sensor operation. This should be
   considered as an option to remove heat generated within the spacecraft bus if
   required

4. The lunar orbit is advantageous at any beta angle to the array cylinder due to
   having no minimum temperature limits. The satellite bus can take advantage of
   the lack of temperature constraints and be designed to utilize the array cylinder as
   a radiator surface.

5. The diameter of the array cylinder will have to take into account the booms and
   extendables on the satellite bus due to the Field of View (FOV) requirement. No

analysis was performed with the bus assumed internal or at the most zenith point of the array cylinder. The FOV concerns can be relieved with careful changes in architecture, but lack of design details and scope prevented investigation.

6. The inner diameter could be increased above the pocketed sensor rows and stiffened and thickened in such a manner to create additional radiator area which would also have a direct view to deep space. The additional area should provide cooler cylinder temperatures due to increased thermal mass, radiator surface area with direct view of deep space and shadowing of the cylinder ID. As sensor temperature is not an issue with any of the cases run, this approach would most likely be utilized in the event that the bus creates an issue due to its own power usage or blockage of radiation paths to space.

With the study complete, it is difficult to argue definitively as to which configuration of cylinder height and diameter would perform the best. Personal experience with satellite design and instrument mounting would suggest that large temperature swings even if below defined maximums cause many problems. Large temperature swings lead to structural movement which will affect pointing knowledge of sensors. Additionally, propulsion, communication and power components cannot function below set temperatures limits. Temperature maintenance for these components will be made more difficult if the system as a whole experiences large temperature fluctuations. With this in mind, the combination of the taller cylinder of moderate diameter (2.2 m as an example) appears the best initial approach for consideration. This is due to both the array and individual sensor temperature swing not being greater than 15 °C during a full orbit.

REFERENCES

Baker, Charles, Christine Cottingham, and Sharon Peabody. "Lunar Reconnaissance Orbiter (LRO) Thermal On-Orbit Performance." *41st International Conference on Environmental Systems.* Portland: AIAA, 2011. 2-4.

Bank, T., and D. Ebbets. *LOCO, Lunar Occultation Observer A First Cut.* September 2009.

Bell, Douglas P, Timothy D Panczak, and Brent A Cullimore. *Thermal Desktop Advanced Modeling Techniques User's Guide.* Manual, C & R Technologies, 2008.

Byers, Bruce K. *Destination Moon: A History of the Lunar Orbiter Program.* Technical Memorandum, Washington: NASA, 1977, 118-120.

Clawson, J. F. et al. "Spacecraft Thermal Environments." Chap. 2 in *Spacecraft Thermal Control Handbook, Volume 1: Fundamental Technologies*, edited by D. Gilmore, 53-55. Reston, Virginia: AIAA, 2002.

Donabedian, M. et al. "Spacecraft Thermal Environments." Chap. 5 in *Spacecraft Thermal Control Handbook, Volume 1: Fundamental Technologies*, edited by D. Gilmore, 161-169. Reston, Virginia: AIAA, 2002.

Falcon 9 Launch Vehicle Payload User's Guides, Rev 1. Hawthorne, CA: Space Corporation Exploration Technologies, 2009.

HEASARC. 2013. https://heasarc.gsfc.nasa.gov/.

Henniger, J. H. "Spacecraft Thermal Environments." In *Spacecraft Thermal Control Handbook, Volume 1: Fundamental Technologies*, edited by D. Gilmore, 791-829. Reston, Virginia: AIAA, 2002.

Luna 3. 2013. http://nssdc.gsfc.nasa.gov/nmc/masterCatalog.do?sc=1959-008A.

Lunar Exploration Timeline. 2011.

      http://nssdc.gsfc.nasa.gov/planetary/lunar/lunartimeline.html.

Lunar Orbiter. 2011. http://nssdc.gsfc.nasa.gov/planetary/lunar/lunarorb.html.

"Lunar Prospector." *National Space Science Data Center.* 1998.

      http://nssdc.gsfc.nasa.gov/nmc/spacecraftDisplay.do?id=1998-001A.

Lunar Reconnaissance Orbiter. 2009.

      http://www.nasa.gov/mission_pages/LRO?mulitmedia/lrocraft5.html.

Lunar Reconnaissance Orbiter Missions. January 2013.

      http://www.nasa.gov/mission_pages/LRO/launch/index.html.

MatWeb, LLC. *MatWeb.* 2012. http://www.matweb.com/refernce/faq.aspx.

Miller, Dr. Richard. 2008.

Miller, R. S. *LOCO-Waggoner.* January 2012.

Miller, R. S. *private communication.* October 2011.

Miller, R.S. *NSF - AAG 2010.* 2010.

Pioneer. 2010. http://space.jpl.nasa.gov/msl/Programs/pioneer.html.

Pioneer 3. 2013. http://nssdc.gsfc.nasa.gov/nmc/spacecraftDisplay.do?id=1958-008A.

Pioneer Space Probes. 2010. http://historicspacecraft.com/Probes_Pioneer.html.

Properties of CsI(Tl). Dynasil. 2010. http://www.hilger-

      crystals.co.uk/properties.asp?material=7 (accessed 2012).

Ranger. 2005. http://nssdc.gsfc.nasa.gov/planetary/lunar/ranger.html.

Ranger 3. 2013. http://nssdc.gsfc.nasa.gov/nmc/spacecraftDisplay.do?id=1962-001A.

Soviet Lunar Missions. 2005. http://nssdc.gsfc.nasa.gov/planetary/lunar/lunarussr.html.

Surveyor. 2006. http://nssdc.gsfc.nasa.gov/planetary/lunar/surveyor.html.

Taurus II User's Manual. Dulles, VA: Orbital Sciences Corporation, 2010.

THERMAL SOFTWARE OVERVIEW

A very brief explanation of the radiation and conduction calculation methodology used by Thermal Desktop® as related to this thesis is provided. Additionally, how radiation interchange calculations are performed is included. The excerpts below are taken directly from Thermal Desktop User's Manual (Bell, Panczak and Cullimore 2008).

Conduction

"For nodes attached to a surface, a thermophysical material is defined…The nodal capacitance is calculated by multiplying the area of the node times the thickness times the specific heat times the density. The capacitance may be constant or temperature varying. If the value is calculated to be zero (i.e. the surface thickness, specific heat, or the density are zero), the node will be output as an arithmetic node…If a node is attached to an element, the capacitance is calculated from the element material and volume. The volume of a planar element is calculated from the area and the thickness…For finite difference surfaces, such as rectangles and cones, the conductors between the nodal regions on a surface are output…using a finite difference formulation. The Galerkin partial differential equation is used to solve the conductance between nodes of a finite element. The equation set representing the heat transfer between nodes is output in…conductor format. Conductors between the same node pairs are added together, if they are of the same type (constant or temperature-varying conductivity). It should be noted that an individual conductor generated by Thermal Desktop for a finite element does not represent the heat transfer between the two nodes referenced by the conductor. The heat

transfer between two nodes is represented by all conductors within the element. For a

complete description of the calculation of element conductivity, please refer to "The

Finite Element Method and Thermal Desktop", that can be found at the CRTech web site

(www.crtech.com) under "Resources"."

Radiation

"RadCAD® uses a stochastic integration technique (often called "Monte Carlo") for

computing radks, dialog box factors, and heating rates. Rays are emitted from each node

and "traced" around the geometry. The rays simulate the effect of a "bundle" of photons.

When a ray strikes another surface, energy is decremented from the ray and absorbed by

the struck surface. The ray is then reflected or transmitted, according to the optical

properties on the surface.

RadCAD also has the option to compute radiation exchange factors from view

factor data (view factors previously computed using ray tracing). A unique progressive

radiosity algorithm is used to iteratively compute radks. The method optimizes

calculations for those view factors that contribute the most to the energy balances for

each node. The currently loaded optical properties are used, allowing radks for different

optical property files to be computed using the same view factor matrix. The method does

not require the view factor matrix to be normalized, since normalization is inherent in the

raytracing and progressive radiosity algorithm.

To compare using Monte Carlo methods for calculation of Radks versus using a

radiosity method from factors, consider a simple cylinder as an example. Suppose that

only the gradient along the length of a cylinder is of interest thermally, but its

participation in the radiation environment is significant. Using RadCAD's Monte Carlo

methods, the cylinder can be nodalized along just the axial direction and accurate results

will be obtained, since RadCAD's raytracing method does not require the condition of

uniform illumination"